AD_____

Award Number: DAMD17-00-1-0476

TITLE: Identification of Structural Domains of ESX Required for Breast Cell Transformation

PRINCIPAL INVESTIGATOR: Arthur Gutierrez-Hartmann, M.D.

CONTRACTING ORGANIZATION: University of Colorado
Health Sciences Center
Aurora, Colorado 80045-6508

REPORT DATE: June 2001

TYPE OF REPORT: Annual

PREPARED FOR: U.S. Army Medical Research and Materiel Command
Fort Detrick, Maryland 21702-5012

REPORT DOCUMENTATION PAGE

Form Approved
OMB No. 074-0188

1. AGENCY USE ONLY (Leave blank)	2. REPORT DATE	3. REPORT TYPE AND DATES COVERED
	June 2001	Annual (1 Jun 00 - 31 May 01)

4. TITLE AND SUBTITLE

Identification of Structural Domains of ESX Required for Breast Cell Transformation

5. FUNDING NUMBERS

DAMD17-00-1-0476

6. AUTHOR(S)

Arthur Gutierrez-Hartmann, M.D.

7. PERFORMING ORGANIZATION NAME(S) AND ADDRESS(ES

University of Colorado
Health Sciences Center
Aurora, Colorado 80045-6508
Email a.gutierrez-hartmann@UCHSC.edu

8. PERFORMING ORGANIZATION REPORT NUMBER

9. SPONSORING / MONITORING AGENCY NAME(S) AND ADDRESS(ES)

U.S. Army Medical Research and Materiel Command
Fort Detrick, Maryland 21702-5012

10. SPONSORING / MONITORING AGENCY REPORT NUMBER

11. SUPPLEMENTARY NOTES

12a. DISTRIBUTION / AVAILABILITY STATEMENT

Approved for Public Release; Distribution Unlimited

12b. DISTRIBUTION CODE

13. Abstract ***(Maximum 200 Words)*** *(abstract should contain no proprietary or confidential information)*

The ESX gene is an Ets member that is potentially very important in breast cancer because the ESX genomic region (chromosome 1q32.1) is amplified in 50% of early breast cancers and ESX mRNA is over-expressed in human breast ductal carcinoma in situ (DCIS). However, the identity, ability and precise molecular mechanism by which any given Ets factor mediates breast cell transformation all remain unknown. The data that we have generated thus far show that ESX, a putative downstream effector of the HER2/neu pathway, regulates expression of the HER2/neu promoter and mediates transformation of MCF-12A human breast cells. Moreover, using the anti-ESX antibody that we generated in collaboration with ABR, Inc, we have shown that the non-transformed MCF-12A cells fail to express ESX, while the transformed and malignant T47D breast cancer cells express abundant amounts of ESX. When we enforce ESX expression in MCF-12A cells, they display increased adhesion, migration and invasion. By contrast, abrogation of endogenous ESX expression in T47D cells via anti-sense or dominant-negative ESX constructs results in a marked reduction of cell growth. Thus, the information gained from these studies has provided critical insights into the mechanisms of ESX-, and therefore of HER2/neu-, mediated breast cell transformation.

14. SUBJECT TERMS	15. NUMBER OF PAGES
Ets, ESX, HER2, neu, ErbB2, transformation, transcription breast cancer	71
	16. PRICE CODE

17. SECURITY CLASSIFICATION OF REPORT	18. SECURITY CLASSIFICATION OF THIS PAGE	19. SECURITY CLASSIFICATION OF ABSTRACT	20. LIMITATION OF ABSTRACT
Unclassified	Unclassified	Unclassified	Unlimited

Table of Contents

INTRODUCTION

The Ets family of transcription factors contains several members that are important components of the cellular pathways leading to tumorigenesis (1). For example, several Ets members are downstream targets of oncogenic Ras (2); dominant-negative Ets reverses the transformed phenotype (3,4); and, Ets proteins have been shown to regulate a repertoire of genes that govern cellular survival, proliferation and migration (1,6). Moreover, several Ets factors have been implicated in breast cancer (1,6). However, the ability of Ets factors to transform human breast cells, the identity of the precise Ets factor required for breast cell transformation, and the molecular mechanism by which such an Ets factor mediates breast cell transformation, all remain unknown. The ESX gene is an Ets member that is particularly relevant to breast cancer. ESX is located on chromosome 1q32.1, in a region that is amplified in 50% of early breast cancers. ESX mRNA is over-expressed in human breast ductal carcinoma in situ (DCIS) (7-9). Also, there is a positive feedback loop between the HER2/neu proto-oncogene and ESX, in that HER2/neu activation induces ESX expression, while ESX activates the HER2/neu promoter via a putative ESX DNA binding site (7-9). Finally, HER2/neu and ESX expression levels are positively correlated in human breast cancer cell lines (7-9). Based on these observations, we have chosen to determine whether ESX is capable of transforming immortalized, but non-transformed MCF-12A human breast cells, and to determine the precise mechanism(s) by which ESX transforms these human breast epithelial cells.

BODY

Task 1: To define the modular structural domains of ESX (± DNA) using Cleveland and peptide sequencing analysis.

We have made diligent progress towards accomplishing this aim. Specifically, we have fully characterized an HA-tagged ESX mammalian expression construct. For example, we have shown that HA-ESX is expressed as a protein of about ~47 kDa; and that HA-ESX stimulates the collagenase and HER2/neu promoters, but fails to activate an intact stromelysin promoter. However, HA-ESX activates, in a dose-dependent manner, a heterologous promoter containing 8 copies of the Ets binding site derived from the stromelysin gene (p8Xpal-CAT). Analysis of the ability of ten Ets constructs to activate the HER2/neu promoter revealed three patterns of gene activation: (1) no effect or repressed promoter activity (Elk-1 and NET); (2) intermediate activity (ER81, GABP, ESX and HA-Ets-2); and, (3) maximal activity (Ets-1, VP-16-Ets-1, and EHF). Using anti-ESX antibodies that we developed (see below), we documented that this differential transcription effects of ESX on various promoters was not due to variable levels of ESX protein expression. Taken together, these data show that HA-ESX differentially regulates several breast-cancer relevant gene promoters, in particular collagenase and HER2/neu.

We have also generated ESX as a fusion protein with GST, and we have optimized conditions to express recombinant GST-ESX in bacteria and to purify it to homogeneity. Using this highly purified recombinant GST-ESX, we have generated rabbit polyclonal anti-ESX antibodies, in collaboration with ABR, Inc., in Golden, CO, as originally proposed. These antibodies, which are very important reagents, are now commercially sold by ABR to

the entire scientific community, thus providing an invaluable research tool to all breast cancer investigators. We have characterized these anti-ESX antibodies and shown that they recognize a ~47 kDa nuclear protein that is expressed in T47D breast cancer cells, but that is not expressed in non-transformed human MCF-12A mammary cells. Additionally, these anti-ESX antibodies have already been very useful in measuring ESX protein expression levels in the transcription and transformation assays, as described above. Finally, we have initiated a new project with these anti-ESX antibodies and we have optimized the chromatin immunoprecipitation (ChIP) assay to show that ESX actually binds to certain cellular target genes in vivo.

Having made GST-ESX containing a thrombin cleavage site between GST and ESX, we have been optimizing conditions for cleavage of ESX from GST-ESX immobilized on glutathione beads. While this approach has been releasing intact ESX, the amounts released are very low (~2-5% of total). Thus, we have had to clone HA-tagged ESX into a variety of other bacterial expression vectors, such as His-tag and an adenoviral mammalian expression vector. This latter approach has been very successful, and we have since documented ESX expression in MCF-12A cells. Thus, we are now ready to initiate the Cleveland digestion steps, as planned.

Task 2: To define the modular domain of ESX required for breast cell transformation.

We have made the most significant progress in this aim and have made several important discoveries about the role of ESX in breast epithelial cell proliferation and transformation. First of all, we have completed the preliminary studies showing that transient expression of HA-ESX and HA-VP16-ESX in MCF-12A cells results in increased colony formation and these data are part of a manuscript recently submitted to Cancer Research (see Appendix). Using a colony formation assay, we found that HA-ESX and HA-Ets-2 mediated MCF-12A cell colony formation rates that approached those generated by oncogenic V12 Ras, whereas empty vector had a negligible effect. By contrast, in immortalized and transformed T47D breast cancer cells, which express abundant amounts of HER2/neu and ESX, we found that anti-sense and dominant-negative HA-ESX inhibited T47D colony formation, whereas control vector allowed formation of many colonies. Finally, we have established a number of MCF-12A cell lines stably expressing either vector control, HA-ESX, HA-VP16-ESX, HA-ETS-2, or V12-Ras. Several of these cells lines have been tested for their ability to grow in an anchorage-independent manner in soft agar. While the positive control, V12-Ras, resulted in a large number of foci, the HA-ESX and HA-Ets-2 stable cell lines also yielded equivalent number of foci, while the vector control lines failed to do so at all. These data indicate that ESX is capable of not only inducing colony formation, but also able to transform MCF-12A cells to levels equal to the strong oncogene V12-Ras. Finally, in collaboration with Dr. Pepper Schedin of the AMC Cancer Center here in Denver, we have determined the adhesion, migration and invasion rates of these various stable cell lines. These data show HA-ESX confers an increased plating efficiency, and migration and invasion rates. In summary, we have accomplished much more towards completing Aim 2.

Task 3: To identify the proteins that associate with the ESX transforming domain using MALDI-TOF.

We have made some initial inroads into this aim as well. For example, we have optimized cell lysis, nuclear extract preparation, and anti-HA immunoprecipitation of HA-tagged ESX expressed from the adenovirus construct.

KEY RESEARCH ACCOMPLISHEMENTS

- Production and characterization of bacterial and mammalian ESX.
- Generation of anti-ESX rabbit polyclonal antibody in collaboration with ABR, Inc.
- HA-ESX differentially activates several breast cancer-relevant gene promoters, including Her2/neu.
- HA-ESX mediates MSF-12A colony formation on tissue culture plates and foci formation in soft agar, and it promotes adhesion, migration and invasion of MCF-12A cells.
- Amino-terminal-truncated and anti-sense ESX constructs abrogate colony formation of transformed T47D cells.
- Establishment of pools of MCF-12A cells stably expressing either HA-ESX, HA-VP16-ESX, HA-Ets2, V12-Ras or vector control.

REPORTABLE OUTCOMES

Abstracts:

(1) Identification of ESX-Regulated Genes that Promote Breast Cell Transformation by cDNA Microarray Analysis, G.J. Cappetta, Kristin Eckel, Arthur Gutierrez-Hartmann, University of Colorado Health Sciences Center, Denver, CO. National Endocrine Society Meeting, Denver, CO, June, 2001.

(2) Analysis of ESX Function in the Development of Human Breast Cancer. J.D. Prescott, A. Gutierrez-Hartmann, University of Colorado Health Sciences, Denver, CO. National Endocrine Society Meeting, Denver, CO, June, 2001.

Manuscripts

(1) K.L. Eckel, J.T. Tentler, G.J. Cappetta, S.E. Diamond and A. Gutierrez-Hartmann. (2001) The epithelial-specific ETS transcription factor ESX/ESE-1/Elf-3 modulates malignancy-associated gene expression and breast cell growth. *Cancer Research*, under revision.

Reagents Developed

(1) Rabbit polyclonal anti-ESX antibodies now commercialized by ABR, Inc., Golden, CO.

Funding applied for and received based on this work

(1) G.J. Cappetta, DOD Pre-Doctoral Award, 2000:not awarded.

(2) G.J. Cappetta, Komen Foundation Pre-doctoral Award, 2001: pending.

(3) J.D. Prescott, Institutional DOD Pre-doctoral Award, 2000: applied and received award.

(4) J.D. Prescott, National DOD Pre-doctoral Award, 6/2001: pending.

CONCLUSIONS

The data that we have generated thus far are of particular significance to breast cancer because we have shown that a putative downstream effector of the HER2/neu pathway, ESX, regulates expression of the HER2/neu promoter and mediates transformation of MCF-12A human breast cells. Moreover, using the anti-ESX antibody that we generated in collaboration with ABR, Inc, we have shown that the non-transformed MCF-12A cells fail to

express ESX, while the transformed and malignant T47D breast cancer cells express abundant amounts of ESX. When we enforce ESX expression in MCF-12A cells, they display increased adhesion, migration and invasion. By contrast, abrogation of endogenous ESX expression in T47D cells via anti-sense or dominant-negative ESX constructs results in a marked reduction of cell growth. Thus, the information that we have gained from these studies have provided novel insights into the mechanisms of ESX-, and therefore of HER2/neu-, mediated breast cell transformation. Ultimately, we anticipate that these studies will provide a novel marker and several new drug targets to use in our battle against breast cancer.

REFERENCES

1. Wasylyk, B, and Nordheim, A. 1997. Ets transcription factors: Partners in the integration of signal responses., p. 251-284. *In* A. Papavassiliou (ed.), Transcription Factors in Eukaryotes. Landes Bioscience.
2. Wasylyk, B, Hagman, J, and Gutierrez-Hartmann, A. 1998. Ets transcription factors: nuclear effectors of the Ras/MAP kinase signaling pathway. Trends Biochem. Sci. 23:213-216.
3. Sapi, E, Flick, M, Rodov, S, and Kacinski, B. 1998. Ets-2 transdominant mutant abolishes anchorage-independent growth and anchorage-stimulating factor-stimulated invasion by BT20 breast carcinoma cells. Cancer Res. 58:1027-1033.
4. Delannoy-Courdent, A, Mattot, V, Fafeur, V, Fauquette, W, Pollet, I, Calmels, T, Vercamer, C, Boilly, B, Vandenbunder, B, and Desbiens, X. 1998. The expression of Ets-1 transcription factor lacking its activation domain decreases uPA proteolytic activity and cell motility, and impairs normal tubulogenesis and cancerous scattering in mammary epithelial cells. J. Cell Sci. 111:1521-1534.
5. Galang, C, Garcia-Ramirez, J, Solski, P, Westwick, J, Der, C, Neznanov, N, Oshima, R, and Hauser, C. 1996. Oncogenic Neu/ErbB-2 increases, Ets, AP-1 and NF-kB-dependent gene expression, and inhibiting Ets activation blocks Neu-mediated cellular transformation. J. Biol. Chem. 271:7992-7998.
6. Janknecht, R, and Nordheim, A. 1993. Gene regulation by Ets proteins. Biochim. Biophys. Acta 1155:346-356.
7. Chang, C, Scott, G, Kuo, W, Xiong, X, Suzdaltseva, Y, Park, J, Sayre, P, Erny, K, Collins, C, Gray, J, and Benz, C. 1997. ESX: A structurally unique Ets overexpressed early during human breast tumorigenesis. Oncogene 14:1617-1622.
8. Oettgen, P, Alani, R, Barcinski, M, Brown, L, Akbarali, Y, Boltax, J, Kunsch, C, Munger, K, and Libermann, T. 1997. Isolation and characterization of a novel epithelium-specific transcription factor, ESE-1, a member of the *ets* family. Mol. Cell. Biol. 17:4419-4433.
9. Tymms, M, Ng, A, Thomas, R, Schutte, B, Zhou, J, eyre, H, Sutherland, G, Seth, A, Rosenberg, M, Papas, T, Debouck, C, and Kola, I. 1997. A novel epithelial-expressed ETS gene, ELF3: Human and murine cDNA sequences, murine genomic organization, human mapping to 1q.32.2 and expression in tissues and cancer. Oncogene 15:2449-2462.

APPENDICES

Enclosed is a draft of a manuscript submitted to *Cancer Research*, which is under revision. It is a total of 63 pages.

K.L. Eckel, J.T. Tentler, G.J. Cappetta, S.E. Diamond and A. Gutierrez-Hartmann. (2001) The epithelial-specific ETS transcription factor ESX/ESE-1/Elf-3 modulates malignancy-associated gene expression and breast cell growth. *Cancer Research*, under revision.

The Epithelial-Specific ETS transcription Factor ESX/ESE-1/Elf-3 Modulates Malignancy-Associated Gene Expression and Breast Cell Transformation

Kristin L. Eckel, John T. Tentler, Gerald J. Cappetta,

Scott E. Diamond[+], and Arthur Gutierrez-Hartmann*

Departments of Medicine and of Biochemistry & Molecular Genetics, Program in Molecular Biology, and Colorado Cancer Center, University of Colorado Health Sciences Center

+ Current Address: Department of Physiology, University of Kentucky College of Medicine, MS-508, Albert B. Chandler Medical Center, 800 Rose Street, Lexington, KY 40536-0298

*To whom correspondence should be addressed: University of Colorado Health Sciences Center, 4200 East Ninth Avenue Box B-151, Denver, CO 80262

Telephone: 303-315-8443

FAX: 303-315-4525

Email: a.gutierrez-hartmann@uchsc.edu

Running Title: ESX modulates breast cell transformation

Abstract

Several members of the ETS family of transcription factors contribute to tumorigenesis in many different tissues, including breast epithelium. The ESX gene is an epithelial-specific Ets member that is particularly relevant to breast cancer. ESX is amplified in early breast cancers, it is over-expressed in human breast ductal carcinoma in situ, and there may be a positive feedback loop between the HER2/neu proto-oncogene and ESX. Despite this progress in our understanding of ESX, its ability to regulate tumor-related gene expression and to modulate breast cell transformation, remain unknown. Here we show that HA-ESX and HA-VP16-ESX, an activated ESX fusion protein, stimulate the collagenase and HER2/neu promoters, but fail to activate an intact stromelysin promoter. However, both HA-ESX and HA-VP16-ESX activate, in a dose-dependent manner, a heterologous promoter containing 8 copies of the Ets binding site derived from the stromelysin gene (p8Xpal-CAT). Analysis of the ability of ten Ets constructs to activate the HER2/neu promoter revealed three patterns of gene activation: (1) no effect or repressed promoter activity (Elk-1 and NET); (2) intermediate activity (ER81, GABP, ESX and HA-Ets-2);

and, (3) maximal activity (Ets-1, VP-16-Ets-1, EHF, and HA-VP16-ESX). Based on these observations, we also determined whether ESX is capable of transforming immortalized, but nontransformed and ESX negative MCF-12A human breast cells. Using a foci formation assay, we found that HA-ESX and, particularly HA-VP-16-ESX and HA-Ets-2, mediated MCF-12A cell transformation rates that approached those generated by oncogenic V12 Ras, whereas empty vector resulted in negligible transformation. By contrast, in immortalized and transformed T47D breast cancer cells, which express abundant amounts of HER2/neu and ESX, we found that anti-sense and dominant-negative HA-ESX inhibited T47D foci formation, whereas control vector allowed formation of many foci. These results are significant because they are the first demonstration of robust transformation by Ets members, and in particular, that HA-ESX and HA-Ets-2 are capable of transforming human mammary cells.

Introduction

The Ets family of transcription factors represents a class of trans-acting phosphoproteins with important roles in cell proliferation, differentiation and oncogenic transformation (1-4). The family is defined by the ETS domain, a highly-conserved DNA-binding domain (DBD) comprised of ~85 amino acids that is folded into a novel winged helix-turn-helix DNA-binding motif (5, 6). Ets proteins function almost exclusively via specific protein-protein interactions, with specific Ets/protein partner combinations binding to bipartite DNA elements on relevant gene promoters (1-4). Thus, the target gene selectivity of Ets factors is greatly influenced by specific protein partners.

The v-*ets* oncogene in the E26 retrovirus causes hematopoetic malignancies in chickens (7). In mammalian cells, Ets proteins are not only key nuclear targets of Ras oncogene signaling pathways, but are also required to trans-activate a subset of genes that initiate cellular transformation. Ets factors, typically acting via the AP-1/Ets Ras reponse element (RRE), regulate a wide repertoire of genes that control cell survival (anti-apoptosis), proliferation and motility, such as: the HER2/neu (8), ß-integrin (9, 10), E-cadherin (11, 12), Bcl-XL (13), cyclin D (14, 15), Fos (1, 16), Myc (17), Ets (Ets-1/2, Pea-3, ESX) (4, 18-22), matrix metalloproteinases (9, 12, 23) and maspin (24) genes. Moreover, Ets-induced malignancies are often due to Ets over-expression or gene translocations resulting in chimeras in which the Ets DBD combines with other activation domains (4). While these data strongly implicate Ets factors and Ets target genes in tumorigenesis

and metastasis, the ability of the *c-Ets-1* and *c-Ets-2* proto-oncogenes to transform NIH 3T3 fibroblasts is actually negligible, and may require a previous "hit" (25-27).

The most compelling data supporting a direct role of Ets proteins in mammary tumorigenesis has been the ability of the dominant-negative (dn) Ets-2 DBD to completely block the anchorage-independent growth and cellular invasiveness of NmuMG, MMT and BT20 breast carcinoma cells (28, 29). The dn-Ets protein functions as a dominant inhibitory effector by competing with endogenous, intact Ets factors for Ets binding sites on target genes (30-36). Moreover, several specific Ets proteins, including members of the ETS-1, PEA-3 and ESX subfamilies, are up-regulated in breast tumorigenesis (12, 21-23). While these studies clearly implicate Ets factors in breast cancer, the ability of a specific Ets factor to actually transform normal breast cells has not been shown.

ESX (epithelial-restricted with serine box), also known as Jen, ERT, ELF-3 or ESE-1, is a novel, epithelial-specific human Ets factor that is unique among Ets factors in several respects (37-41). First, its expression is restricted to the most terminally-differentiated epithelial-derived cells in the colon, prostate, kidney, uterus, skin, pancreas, stomach, trachea, fetal lung, and the mammary gland (20, 40). Second, ESX contains not only the usual Pointed (PNT) and ETS DBD domains

found in many Ets factors, but also contains a Sox-like serine-rich box and an HMG-like AT-hook domain (Fig. 1) (20, 37, 39-42).

ESX is of particular relevance to breast cancer. ESX expression in normal breast increases in the epithelium of ductules and terminal ductal-lobular units during ductal development, then declines throughout terminal differentiation, and is then re-expressed dramatically during glandular involution (20). Thus, ESX expression in normal breast may be involved in the restructuring and involution processes of the mammary gland, and aberrant ESX expression may alter these normal breast re-modeling processes and result in tumorigenesis (20). Indeed, ESX is abundantly expressed in human mammary epithelial carcinomas (37, 41). Moreover, the ESX gene maps to human chromosome 1q32.1, in a region that is over-represented in 50% of early breast cancers (37, 41). Additionally, ESX is over-expressed in human breast ductal carcinoma in situ (DCIS) (37); an early cancer stage that also over-expresses HER2/neu (43). A positive feedback loop between the HER2/neu proto-oncogene and ESX appears to exist in human breast cancer cell lines (20, 37). Thus, taken together, these data show that ESX is a critical gene target of the HER2/neu pathway, and suggest that ESX expression may be necessary to achieve the particularly malignant phenotype associated with HER2/neu.

Here we show that HA epitope-tagged ESX and VP16-ESX, an activated form of ESX, stimulate certain metalloproteinase genes and the HER2/neu promoter, and that the HER2/neu promoter is differentially activated by ten distinct Ets transcription factor consteucts. Most importantly, we show that HA-ESX, HA-VP16-ESX and HA-Ets-2 are able to transform MCF-12A human breast cells with equal potency as oncogenic V12Ras, and that anti-sense and dominant-negative HA-ESX inhibited T47D foci formation. These results are significant because they are the first demonstration of unambiguous transformation of human mammary cells by members of the Ets family of transcription factors.

Materials and Methods

ESX mammalian expression vectors- A cDNA spanning the coding sequence of human ESX mRNA was amplified by RT-PCR using oligonucleotides directed to the 5' and 3' ends of the ESX open reading frame, to produce an ESX DNA product flanked by *BamH* I and *EcoR* I sites for later subcloning. The ESX oligonucleotide sequences used were:

5' cgagatctccggaattcatATGGCTGCAACCTGTGA and

5' tccagagtcggaactgaatGAATTCCGGAGATCTCG, with the capital letters indicating ESX sequences and underlined bases representing the ATG in the first sequence. Amplified ESX cDNA was subcloned into pCR2.1 (Invitrogen Corporation) to yield pCR2.1-ESX plasmid DNA. The ESX

sequence and its orientation was verified by dideoxy sequencing by the UCHSC Cancer Center DNA Sequencing Core facility. Plasmid pCR2.1-ESX was used as the source of ESX DNA for the construction of a variety of mammalian ESX expression vectors. Thus, ESX was excised from pCR2.1-ESX by digestion with *EcoR* I and ligated to the unique *EcoR* I site of mammalian expression vector pCDNA3.1 (Invitrogen Corporation) to generate pCDNA3.1-ESX. Similarly, pCR2.1-ESX was digested with *Bgl* II and *Afl* III, and the 1116 base pair *Bgl* II ESX fragment was ligated into a *BamH* I linearized and dephosphorylated pCGN2-HA vector (44-46) to generate pCGN2-HA-ESX. The pCGN2-HA-VP16-ESX plasmid was constructed by first amplifying amino acids 3 to 72 from the viral VP16 trans-activation domain (TAD) from pGAL4-VP16, using the following oligonucleotide primers: 5' aagcttcGGCCCCCCCGACCGATGTCAGC and 5' ccatggCATCGGTAAACATCTGCTC (Gibco/BRL). The resulting DNA fragment was cloned into pCR2.1, generating plasmid pCR2.1-VP16, and its DNA sequence was verified as described above. The VP16 TAD and fifteen 5' flanking base pairs were excised from pCR2.1-VP16 using *EcoR* I. DNA ends were blunted using the Klenow fragment of DNA polymerase, and the resulting fragment was then cut with *Hind* III to remove vector sequences from the 5' end and to provide appropriate reading frame. This *Hind* III/blunt-ended VP16 fragment was then ligated into a *Hind* III and *Sma*I-cut pCGN2-HA-ESX plasmid, such that the VP16 TAD was inserted between the HA tag and the N terminal end of ESX to produce pCGN2-HA-VP16-ESX. Construction of the dominant-negative version of ESX was accomplished in two cloning steps. First, the ESX AT-hook

and DNA binding domain was PCR amplified from pCR2.1-ESX, using an oligonucleotide that included a Kozak consensus site (lower case), followed by an initiator methionine (bold), an in-frame HA epitope tag (italics) and a five amino acid linker (underlined) fused to amino acid 270 of ESX:

5' ccacc**ATG***GCTTCTTATCCTTATGACGTGCCTGACTAT*GCCAGCTCGGGACCTGATG GTTTTGGTGAC 3'. The same 3' primer that was used for the construction of pCR2.1-ESX was also used for the amplification of the ESX DBD region. The PCR product was cloned into pCR2.1 and the DNA sequence was verified by the UCHSC core sequencing facility. In the second cloning step, the HA-ESX DBD cDNA was excised from pCR2.1-ESX DBD with *EcoR* V and *Spe* I and sub-cloned into pCDNA3.1 at the *EcoR* V and *Xba* I sites, resulting in a dominant-negative version of ESX, (pCDNA3.1-HA-ESX DBD).

Reporter constructs- The 1100-CAT and 550-CAT, contain 1100 and 550 bp of upstream promoter sequences derived from the rat stromelysin gene, respectively, and have been described previously (47). The –517pBLCAT collagenase construct contains the -517 to +63 region of the human collagenase gene cloned in the pBLCAT plasmid (48). The pA3Her2/neu-Luc reporter was constructed by first amplifying the -582 to +30 region of the human Her2/neu promoter region from HeLa genomic DNA using the following primers (Gibco/BRL): 5' AAGTCCTTTCGATGAGACT 3' and 5' AAGCTTCTGGTTTCTCCGGTCCCAATGGA 3'. This 612 bp fragment, which included

an internal, genomic Sma I site at position, was cloned in to pCR-2.1. Once its DNA sequence was verified, a 527 bp fragment spanning positions -497 to +30, was excised from pCR2.1-Her2/neu and then ligated directionally into the *Hind* III and *Sma* I sites of the luciferase based reporter vector, pA3luc (49).

Ets factor and Ras effector plasmids- Ets factor plasmids pTL1-Elk-1, pSG5-Ets-1, pSG5-VP16-Ets-1, and pTL2-hNet constructs were provided by Bo Wasylyk (IGBMC, Illkirch, France) and the HA-tagged Ets-2 (pCGN-HA-Ets-2) was provided by Michael Ostrowski (Ohio State University). EHF, ER81 and GABP plasmid constructs were provided by Frank Burton (University of Minnesota), Ralf Janknecht (The Salk Institute) and Tom Brown (Pfizer, Inc.), respectively. Plasmid pSV-Ras contains oncogenic V12-Ha-Ras and was provided by Robert Weinberg (Massachusetts Institute of Technology).

Cell Culture- Human HeLa cells and T47D breast cancer cells were grown in Dulbecco's modified Eagle medium (DMEM, Life Technologies, Inc.) containing 12.5% horse serum, 2.5% fetal calf serum, and 50 μg/ml of penicillin and streptomycin (Gibco/BRL). The MCF-12A cell line was grown in Ham's F12/DME media supplemented with 5% horse serum, 100 ng/ml cholera toxin (Gibco BRL), 10 μg/ml insulin (Sigma), 0.5 μg/ml hydrocortisone (Sigma), 20 ng/ml EGF (Sigma) and 50 μg/ml of penicillin and streptomycin (GibcoBRL). All cells were grown at 37°C in 95% O_2

and 5% CO_2. Cells were passaged regularly at 70-80% confluence by harvesting in 1x PBS and 3 mM EDTA before re-plating in fresh media.

CAT assays- HeLa cells were grown to 60-80% confluence and then harvested in 0.05% trypsin and 0.5 mM EDTA (Gibco BRL) and resuspended in DMEM supplemented with 12.5% horse and 2.5% fetal calf serum to a concentration of $5x10^6$ cells per ml. Plasmid DNA was mixed with approximately $1x10^6$ cells in a volume of 200 μl, and electroporated at 220 volts and 500 μFd using a Bio-Rad Gene Pulser. Cells were incubated for 24 hours in regular growth media before harvesting for CAT assays. After 24 hours, cells were harvested with 1x PBS and 3 mM EDTA, pelleted, and lysed in 0.1 M $KHPO_4$ and 0.1 M DTT. Cellular debris was removed by centrifugation and the protein concentration in the supernatant was measured using the Bradford method. CAT assays were performed using 115 μg of protein, 20 μl of 3.3 mg/ml acetyl CoA (Boehringer Mannheim), and 10 μl of 1:10 diluted [^{14}C]-chloramphenicol (56 mCi/mmol). The volume of each reaction was normalized to 150 μl with 0.25 M Tris HCl (pH 7.8) and extracts were incubated for one hour at 37°C before the addition of 20 μl of fresh acetyl CoA. Reactions were incubated for one more hour and then stopped by the addition of 800 μl of ethyl acetate. The organic phase was concentrated in a speed vacuum microcentrifuge for 30 minutes on medium heat (43°C) and the resulting pellet was resuspended in 25 μl ethyl acetate. The resuspended pellet was spotted onto Silica Gel 60 TLC plates (Selecto Scientific) and thin layer chromatography was performed in 95%

chloroform and 5% methanol. CAT activity was calculated based on the amount of ^{14}C that was incorporated into acetylated chloramphenicol, as quantified by a Phophor Imager (Molecular Dynamics). Duplicate results were averaged together and the standard deviation was calculated for each set of duplicates.

Luciferase Assays- HeLa cells were grown to 60-80% confluence and then trypsinized, counted and plated in 96 well plates at a density of 4 x 10^4 cells per well. Cells were then transfected with 100 ng of the pA3Her2/neuLuc reporter plasmid, 1 ng of a Renilla luciferase plasmid (Promega) and 10, 30, 60, or 100 ng of the effector plasmids. Transfection was done according to the protocol provided with the Effectene Transfection Reagent kit (Qiagen). Sixteen hours after transfection, the media was replaced with fresh media. Twenty hours after transfection, cells were rinsed with 1x PBS and then lysed directly on the plate with 1x Passive Lysis Buffer (Promega). Cells were allowed to incubate for 15 minutes in lysis buffer before the lysates were transferred to a 96 well Microlite plate (Dynex Technologies). Light units for the Her2/neu-Luc and Renilla luciferase expression were read using an MLX Microtiter Plate Luminometer (Dynex Technologies) and a Promega Dual Luciferase Reporter Assay System (Promega).

Immunoprecipitations- HeLa cells transfected with 10 μg of either pCGN2-HA-ESX, pCGN2-HA-VP16-ESX or pHA-MAPK were rinsed with ice cold 1x PBS on the plate, and then lysed on the

plates by adding 200 μl of 55 mM TEA (pH 7.5), 111 mM NaCl, 2.2 mM EDTA, 1 mM EDTA, and 0.44% SDS at room temperature, and using a cell scraper. The lysate was collected, vortexed vigorously for five seconds, and then incubated at 68°C for 10 minutes, followed by a 25 minute incubation on ice. Each lysate was adjusted to 1.2% Triton by the addition of 65 μl of a 10% Triton X-100 solution to each tube. Immunoprecipitation was performed using 1 μg of a monoclonal antibody to HA (BAbCO, Inc.) and 65 μl of a slurry of protein A/G agarose beads (Santa Cruz Biotechnology). Protein was allowed to immunoprecipitate for 16 hours at 4°C. The beads were spun down and washed twice with a buffer containing 50 mM TEA, pH 7.5, 100 mM NaCl, 2 mM EDTA, 0.1% SDS, 0.5% Triton X-100 and twice with 10mM TEA pH 7.5. One hundred μl of a commercial 2x SDS protein load dye containing 0.25 M Tris/HCl pH 6.8, 2% SDS, 10% β-mercaptoethanol, 30% glycerol, 0.01% bromophenol blue (Owl Separation Systems) was added to the protein A/G agarose beads in each tube. Samples were then vortexed, boiled for five minutes to release the immunoprecipitates from the beads, and the supernatants loaded onto a 10% PAGE gel. Immunoprecipitated protein bands were visualized by Western blot analysis.

Western Blot Analysis- Protein was transferred from the polacrylamide gel onto nitrocellulose by electrotransfer. The nitrocellulose membrane was incubated for one hour with 5% milk and 0.2% Tween 20 in 1X PBS (blocking buffer) before being probed overnight with a monoclonal HA antibody (BAbCO, Inc.) at a dilution of 1:1000 in blocking buffer. Membranes were then probed

with goat-anti-mouse-HRP secondary antibody (Santa Cruz Biotechnology) in blocking buffer, for one hour at a 1:5,000 dilution. Protein bands were then detected using enhanced chemiluminescence (ECL) (Amersham Pharmacia Biotech), according to manufacturer's directions.

MCF-12A Foci Assays- Immortalized MCF-12A cells were grown in Ham's F12/DME media containing 100 ng/ml cholera toxin (Gibco BRL), 20 ng/ml EGF (Sigma), 10 μg/ml insulin (Sigma), 5% horse serum (Gibco BRL), and 0.5 μg/ml hydrocortisone (Sigma). Cells were grown to approximately 80% confluence before being harvested with trypsin/EDTA and pelleted. Cell pellets were resuspended in complete media and approximately $4x10^5$ cells were electroporated at 960 μFd and 220 volts in a volume of 200 μl with 10 μg of either empty vector pCGN2, pCGN2-HA-ESX, pCGN2-HA-VP16-ESX, pCGN-HA-Ets-2, or pSV Ras. Two thousand cells were plated in complete media in triplicate in 60 mm tissue culture dishes and grown in 95% 0_2 and 5% CO_2 at 37°C. Media was changed every 2-3 days for the duration of the incubation. On the thirteenth day of incubation, colonies were rinsed with 1x PBS and fixed with a graded methanol series of 50%, 70%, 90%, 95% and 100% methanol for five minutes each. Fixed cells were then stained for 5 minutes with Wright's stain (Sigma), followed by a 10 minute incubation in a 1:10 dilution of Giemsa stain (Sigma). Colonies were rinsed several times with H_2O in order to reduce background stain and then photographed and counted manually based on a colony size that was greater than 1 mm in diameter.

T47D Foci Assays- Human T47D breast cancer cells were harvested at approximately 70-80% confluence in 0.05% trypsin and 0.5 mM EDTA. Cells were spun and resuspended in DMEM containing 12.5% horse serum and 2.5% fetal calf serum to a concentration of approximately 1 x 10^6 cells per 200 μl volume. Cells were co-transfected in a 200 μl volume with 2 μg of a plasmid containing green fluorescent protein (EGFP, Clontech) and 20 μg of plasmids encoding for either anti-sense ESX (pCGN2-HA-anti-ESX), dominant-negative ESX (pCDNA3.1-HA-ESX DBD), or empty vector (pCGN2) by electroporation and plated in 60 mm plates. Twenty-four hours post-transfection, cells were harvested with 1 x PBS and 3 mM EDTA and were spun down before resuspending in media for flow-cytometric analysis. Flow-cytometric analysis was performed in sterile conditions to select for green fluorescent cells with a FACScan fluorescent-activated cell-analyzer at the University of Colorado Health Sciences Center Flow-Cytometric Core Facility. Two thousand sorted, green-fluorescent cells were seeded in 60 mm dishes in 3 ml of complete growth media containing 12.5% horse serum and 2.5% fetal calf serum. After cells had adhered to the plate, media was removed and fresh media with 0.1%, 1%, or 5% serum was added to the cells. Cells were allowed to incubate for 13 days during which the media was replaced every two days. On day 13, plates were rinsed with 1 x PBS and then fixed and stained using Crystal Violet (Sigma). Foci were counted manually.

Results

Construction of HA-ESX and HA-VP16 ESX expression vectors

The human ESX gene consists of nine exons and eight introns that span approximately 4 kb of DNA on chromosome 1q32, and encodes a 371 amino acid protein product that is reported to be 42 kDa in mass (37). The ESX protein is comprised of multiple functional domains, including an N-terminal pointed (PNT) domain, a serine box, an AT-rich region and a C-terminal ETS DNA binding domain (ETS-DBD) (Fig. 1A). Additionally, deletion analysis has identified a highly acidic trans-activation domain (TAD) spanning amino acids 129 and 159 (50). In order to study the transcription and transformation properties of ESX, full-length ESX was amplified by RT-PCR from T47D mRNA and then amino-terminally tagged with the hemagglutinin (HA) epitope by cloning into the pCGN2 mammalian expression vector (pCGN2-HA-ESX, Fig 1B) (44, 45). The HA epitope tag was included in order to monitor ESX expression levels, as there were no available antibodies directed to ESX. Furthermore, it enabled us to distinguish between recombinant ESX and the endogenous protein. Additionally, a second ESX expression plasmid was created, pCGN2-VP16-ESX, which includes amino acids 3 to 72 of the viral VP16 transactivation domain (TAD) inserted in-frame between the HA tag and the ESX coding region in pCGN2-HA-ESX (Fig. 1C). This was constructed to generate an ESX protein with enhanced transcriptional activity. The VP16

TAD enhances transcription by recruiting proteins into a pre-initiation complex with RNA polymerase II (50).

Expression of HA-ESX and HA-VP16ESX Protein

In vitro transcription and translation reactions were performed in order to determine the molecular weight at which ESX migrates on SDS-polyacrylamide gels. Translation products labeled with S^{35}-methionine were separated by electrophoresis on a 10% polyacrylamide gel, blotted onto a nitrocellulose membrane and detected by autoradiography (Fig. 2). As a negative control, the reticulocyte lysate reaction was carried out in duplicate in the absence of input DNA and no specific translation product was detected (Fig. 2, lanes 1 & 2). As a positive control, the reticulocyte lysate assay was performed in duplicate with chicken Ets-1 DNA, and the predicted 68 kDa protein product was consistently noted as a doublet (Fig. 2, lanes 3 & 4). In vitro transcription and translation of pCDNA3.1-ESX plasmid, also performed in duplicate, resulted in a protein migrating at 47 kDa (Fig. 2, lanes 5 & 6). Contrary to theoretical size calculations, which predict a size of 42 kDa for ESX protein, we determined ESX migrated at 47 kDa by plotting the relative migration (Rf) of the protein vs. the log of the molecular weight. This was done by analyzing gels of various polyacrylamide percentages to verify the 47 kDa migration pattern of ESX (data not shown).

To further confirm the proper expression and size of ESX and VP16-ESX proteins in vivo, plasmid constructs expressing HA-tagged versions of these two ESX proteins (pCGN2-HA-ESX and pCGN2-HA-VP16-ESX) were transiently transfected into HeLa cells. ESX was immunoprecipitated from transfected HeLa cell lysates using a monoclonal anti-HA antibody (BAbCO), immunoprecipitates were separated by polyacrylamide gel electrophoresis, and the HA-tagged ESX was detected by Western blot analysis using an anti-HA antibody. Figure 3 shows that transfection of the empty vector control plasmid, pCGN2, resulted in no detectable expression of any HA-containing protein (lane 2). By contrast, HeLa cells transfected with the pCGN2-HA-ESX produced a 48 kDa protein (Fig. 3, lane 3), which is consistent with the migration of 47 kDa for ESX plus the 1 kDa contributed by the HA tag. Similarly, HeLa cells transfected with pCGN2-HA-VP16-ESX produced a protein product that migrated at about 56 kDa (Fig. 3, lane 4), which is larger than HA-ESX due to the addition of the 8.4 kDa from the VP16 trans-activation domain plus the 1 kDa of the HA tag. Of note, the expression of HA-ESX was more efficient than that of HA-VP16-ESX, despite equal DNA inputs, and this pattern was also noted in Western blot analysis of whole cell extracts that were not immunoprecipitated (data not shown). As a positive control and to serve as a size standard, we also transfected cells with pHA-42MAPK. As shown in Fig. 3, lane 5, HA-42MAPK is expressed well, migrates at the 42 kDa size by Rf analysis, and runs well below HA-ESX, further indicating that HA-ESX is not migrating at 42 kDa.

Transcriptional Potency of HA-ESX and HA-VP-16-ESX

Having shown that HA-ESX and HA-VP16-ESX are expressed after transient transfection, we next sought to determine their relative transcription potencies. We used the 8xpal-pBLCAT as a reporter construct, since it contains eight copies of an Ets binding site derived from the rat stromelysin promoter (47). HeLa cells were transfected in duplicate with 4 μg of the empty vector control, pCGN2, and only minimal amounts of CAT activity were detected (Fig. 4A, lanes 1 & 2, and Fig.4B). Duplicate transient transfections with increasing amounts of pCGN2-HA-ESX DNA resulted in a dose-dependent increase in 8xpal-pBLCAT transcription activity, with 1, 2 and 4 μg of pCGN2-HA-ESX DNA resulting in 3.2%, 6.2%, and 14.9% conversion to acetylated chloramphenicol, respectively, reflecting CAT activity (Fig. 4A, lanes 3-8, and Fig. 4B). Duplicate transfection of the same doses of pCGN2-HA-VP16-ESX resulted in 6.4%, 11.7%, and 21.2% conversion to acetylated chloramphenicol (Fig. 4A, lanes 9-14, and Fig. 4B). Finally, duplicate transfection of 2 μg of either pCGN2-HA-Ets-2 or of pSVRas, as positive controls, resulted in 7.8% and 10.1% conversion to acetylated chloramphenicol, respectively (Fig. 4A, lanes 15-18, and Fig. 4B). Thus, HA-VP-16-ESX is about 2-fold more active than HA-ESX on this particular reporter construct.

Differential Activation of Metalloproteinase Promoters by ESX

Matrix metalloproteinase genes have been shown to be key targets of Ets proteins, and it has been suggested that the Ets-mediated induction of these genes contributes to the invasive and angiogenic phenotypes of malignant cells (9, 12, 23). While HA-ESX and HA-VP16-ESX were capable of activating the 8xpal pBLCAT reporter construct, it should be noted that this is an artificial promoter construct containing eight copies of the stromelysin Ets binding site (EBS) fused upstream of a minimal TK promoter (47). Therefore, we next determined the ability of HA-ESX and HA-VP16-ESX to activate the EBS in the context of the authentic stromelysin promoter, and whether these Ets factors could activate other metalloproteinase promoters. Figure 5A (lanes 1 & 2) and Fig. 5B, show that the activity of the rat -1100 stomelysin promoter transfected into HeLa cells is minimally detectable (2.5% conversion to acetylated chloramphenicol). Surprisingly, pCGN2-HA-ESX, pCGN2-HA-VP16-ESX and pCGN2-HA-Ets-2 (10 μg each) failed to activate the –1100 rat stromelysin promoter (Fig. 5A, lanes 3-8, and Fig. 5B). Furthermore, doses of pCGN2-HA-ESX ranging from 0.1 to 20 μg failed to produce CAT activity at any dose, suggesting that the lack of stromelysin promoter activity was not due to squelching effects or to insufficient expression of this construct (data not shown). By contrast, 10 μg of pSV Ras and pSG5c-Ets-1 caused robust activation of the -1100 rat stromelysin promoter (Fig. 5A, lanes 9-12, and Fig. 5B), showing that this reporter is functional. Moreover, this lack of transcriptional effect of HA-ESX, HA-ESX-VP16-ESX and HA-Ets-2 is not due to the presence of a TGFß inhibitory element (TIE) on the rat

–1100 stromelysin promoter, since similar analysis of a truncated rat stromelysin promoter (-550-CAT) lacking the TIE (TGF-beta inhibitory element) was used to determine potential changes in activation by HA-ESX, HA-VP16-ESX, HA-Ets-2, c-Ets-1, and V12-Ras on a promoter without the TIE. While V12-Ras activation of the –550 stromelysin promoter appeared to be less than that of the –1100 promoter, no other significant differences were noted in the activation pattern of the shortened rat stromelysin promoter (data not shown).

To further determine the role of ESX in metalloproteinase gene activation, we chose to investigate whether ESX could activate the collagenase promoter, which also contains an Ets binding site. Here, we show that HA-ESX, HA-VP16-ESX, and HA-Ets-2 were capable of activating the -517 to +63 region of the human collagenase promoter (Fig. 6). Like the stromelysin promoter, the human collagenase promoter had no detectable basal activity when transfected into HeLa cells (Fig. 6A, lanes 1 & 2, and Fig. 6B). Moreover, transfection of empty vector had no effect on basal collagenase promoter activity, whereas HA-ESX resulted in a dose-dependent and strong activation of this reporter. As shown in Fig. 6A, lanes 3-8, and quantitated in Fig. 6B, HA-ESX resulted in 2.2%, 13.5%, and 44.5% conversion to acetylated chloramphenicol at 1, 5 and 10 μg of DNA input, respectively. HA-VP16-ESX also activated the collagenase promoter, resulting in 7.2%, 3.4% and 12.7% conversion to acetylated chloramphenicol at 1, 5 and 10 μg of DNA input, respectively (Fig. 6A, lanes 9-14, and Fig. 6B). This level of activation is significantly less than that

obtained with HA-ESX (Fig. 6A, lanes 3-8, and Fig. 6B). Finally, the two positive controls, human HA-Ets-2 (10 μg) and V12-Ras (10 μg), mediated robust activation of the collagenase promoter, resulting in 28.6% and 33.2% conversion to acetylated chloramphenicol, respectively (Fig. 6A, lanes 15-18, and Fig. 6B).

Response of the Her2/neu promoter to ten distinct Ets factor constructs

Over-expression of the Her2/neu proto-oncogene is found in about 30% of human breast cancers, and this overexpression is thought to contribute to mammary tumorigenesis (43). Furthermore, the proximal region of the Her2/neu promoter contains a functional Ets binding site immediately upstream of the TATA-box, at position –26, that has been show to respond to co-transfected PEA3 (22, 51) and ESX (8, 37) in transient transfection reporter assays. Since multiple Ets factors have been shown to be expressed in breast cancer cell lines (8, 12, 21, 23, 37, 52), the precise identity of the specific Ets factor that activates the Her2/neu promoter in vivo remains unknown. Thus, we chose to test the ability of increasing doses of ten distinct Ets factor constructs to activate the Her2/neu promoter, in order to determine the relative transcription potencies of these Ets factors on the Her2/neu promoter. The -497 to +30 region of the human Her2/neu promoter region was cloned into a luciferase reporter plasmid (pA3Luc) and the effects of Elk-1, ER-81, c-Ets-1, VP16-Ets-1, NET, GABP, EHF, HA-ESX, HA-VP16-ESX and HA-Ets-2 on the Her2/neu promoter was examined (Fig. 7). The results were grouped according to the mammalian expression

vector used to drive these various Ets factors. Figure 7A shows those driven by an SV40 promoter-based vector (Elk-1, ER81, and VP16-Ets-1), and Figure 7B shows those driven by CMV promoter-based vectors (NET, GABP, EHF, HA-ESX, HA-VP16-ESX and HA-Ets-2).

For the SV40 promoter-driven Ets factors, pSG5 was used as the empty vector (47). Increasing doses of an empty pSG5 vector had minimal effects on the activity of the Her2/neu promoter, whereas Elk-1 resulted in a strong dose-dependent reduction in promoter activity (Fig. 7A). In contrast, ER81, Ets-1, and VP16-Ets-1 all resulted in activation of the Her2/neu promoter. Of note, ER81 resulted in a modest ~2-fold response of the Her2/neu promoter at the lowest DNA input, and this response was completely abrogated with increasing doses of ER81 input DNA (Fig. 7A). All doses of c-Ets-1 and VP16-Ets-1 activated the Her2/neu promoter nearly equally, with c-Ets-1 mediating an average ~5.5-fold response and HA-VP16-Ets-1 mediating an average ~6-fold response (Fig. 7A). Finally, V12-Ras produced about a 2-fold activation of the Her2/neu promoter at all doses tested (Fig. 7A).

For the CMV promoter-driven Ets factors, pCGN2 (44, 45) was used as the CMV promoter-containing, empty vector control. As shown in Fig. 7B, increasing doses of pGGN2 had no significant effects on the activity of the Her2/neu promoter. By contrast, NET, a repressor Ets transcription factor, inhibited Her2/neu promoter activity by approximately 50%, compared to

vector-only controls (Fig. 7B). GABP (containing equal amounts of GABPα and GABPβ) resulted in a ~3.5-fold response at the lowest DNA dose, and this effect was eliminated completely with increasing doses of input DNA. EHF mediated an ~8.5-fold response of the Her2/neu promoter, which was also reduced in a DNA dose-dependent manner. However, EHF maintained a ~3-fold effect at the highest DNA dose (Fig. 7B). HA-ESX resulted in a ~3.5-fold response at the first three doses of input effector DNA, and this response was reduced slightly to a ~2-fold effect at the highest input DNA. HA-VP16-ESX resulted in a similar response, averaging about a 4-fold response at the first three input DNA doses, and a stronger ~9-fold response at the highest input DNA dose. Finally, HA-Ets-2 mediated a ~4-fold response at the lowest input DNA, and then stabilized to a 2.5-fold response at the subsequent three higher input DNA doses (Fig. 7B). These data show that the Her2/neu promoter responds differentially to distinct Ets family members. Specifically, the HER2/neu promoter revealed three patterns of gene activation by these ten distinct Ets factor constructs: (1) no effect or repressed promoter activity (Elk-1 and NET); (2) intermediate activity (ER81, GABP, HA-ESX and HA-Ets-2); and, (3) maximal activity (Ets-1, VP-16-Ets-1, EHF, and HA-VP16-ESX).

ESX positively modulates foci formation in MCF-12A cells

Having established the ability of HA-ESX and HA-VP16-ESX to transcriptionally activate promoters involved in tumorigenesis, we chose to determine whether ESX could function as a

transforming factor. To accomplish this, the immortalized but nontransformed human breast epithelial cell line, MCF-12A, was used to evaluate the transforming capabilities of HA-ESX, HA-VP16-ESX, HA-Ets-2, and V12-Ras in foci formation assays. MCF-12A cells were transfected with the empty vector (pCGN2) or the various Ets constructs, plated at a low density in complete Ham's F12/DME media and cultured for 13 days prior to staining the foci. Foci were measured and all foci greater than 1mm in diameter were counted. Figure 8A shows results from a representative experiment performed in duplicate revealing that empty vector resulted in a negligible number of foci, whereas the positive V12-Ras control resulted in a much larger number of foci. In this same assay, HA-VP16-ESX also resulted in a large number of foci, and these foci appeared to be qualitatively similar to those generated by oncogenic V12-Ras.

In order to obtain a more complete and quantitative analysis of the foci-forming ability of the various Ets constructs, Fig. 8B shows the results of a similar study performed in triplicate using pCGN2, pCGN2-HA-ESX, pCGN2-HA-VP16-ESX, pCGN2-HA-Ets-2 and pSV Ras. Again, the negative pCGN2 control formed a minimal number of foci, averaging 6 foci/plate, and the positive control, oncogenic V12-Ras, resulted in a higher number (~32 foci/plate) of foci over 1mm in diameter (Fig. 8B and Table 1). The HA-ESX and HA-VP16-ESX resulted in ~17 and ~20 foci/plate, respectively, which is about 3- and 5-fold greater than the vector clone results (Fig. 8B and Table 1). As with the previous study shown in Fig. 8A, the ability of HA-VP16-ESX and V12-

Ras to form foci were quite similar (~20 vs ~32 foci/plate). Finally, HA-Ets-2 revealed an ability to form foci in MCF-12A cells, resulting in ~23 foci/plate, which is similar to HA-ESX and HA-VP16-ESX (fig. 8B and Table 1), however, HA-Ets-2 appeared competent to efficiently induce many foci smaller than 1mm in diameter.

Anti-sense ESX and dominant-negative ESX suppress foci formation of T47D human breast cancer cells

Based on the ability of HA-ESX and HA-VP16-ESX to induce foci formation in MCF-12A cells, we chose to test the role of endogenous ESX in foci formation in transformed T47D human breast cancer cells, since this cell line expresses easily detectable levels of ESX protein (data not shown). To this end, we transfected T47D cells with pGFP and either HA-antisense-ESX or a dominant-negative HA-ESX DBD (containing only the AT-hook and DNA-binding domains) in a 1:10 ratio and selected for the transfected population by FACS for GFP fluorescence. This enriched population of transfected cells was then plated in various concentrations of serum (0.1%, 1% and 5%), and foci formation was recorded (Fig. 9) and quantitated (Table 2) 13 days later, as described in the Methods section. As shown in Fig. 9, T47D cells transfected with empty vector control resulted in numerous cell colonies, ranging from 301-326, at all serum concentrations (Table 2). Indeed, the effect of increasing serum concentration primarily affected colony size in these empty vector controls (Fig. 9). By contrast, T47D cells transfected with antisense ESX resulted in a

significant reduction in foci formation, resulting in 67, 82 and 126 foci at 0.1, 1 and 5% FCS, respectively. Compared to the empty vector results at each equivalent serum concentration, these numbers represent 22, 28 and 39% colony forming efficiency, respectively (Table 2). Finally, T47D cells transfected cells with a truncated dominant-negative version of ESX reveals similar reductions in foci formation, resulting in 52, 67 and 146 foci at 0.1, 1 and 5% FCS, respectively, (Fig. 9 and Table 2). These data represent 17, 22 and 45% colony forming efficiency at 0.1, 1 and 5% FCS, respectively, compared to vector controls (Fig. 9 and Table 2).

Discussion

Although a number of studies have implicated several Ets family members in mammary tumorigenesis, the precise role of any specific Ets factor in breast cancer remains unknown. In this study, we show that the epithelial-specific Ets family member, ESX, is expressed from mammalian expression vectors resulting in a protein of about ~47 kDa that is able to differentially activate several promoters, including the collagenase promoter, and to mediate foci formation of MCF-12A nontransformed mammary cells. In addition, anti-sense and dominant-negative ESX reduces clonagenic growth of T47D transformed breast cells. Thus, we have shown by several different approaches that ESX modulates the expression of malignancy-associated genes and of breast cell transformation. These results are significant in that they provide the first evidence of potent cell transformation by any Ets factor and, specifically, because they show that Ets factors can transform mammary cells in culture.

ESX is expressed as a 47 kDa protein in vitro and in vivo

Two distinct cDNA clones for human ESX have been isolated, differing in length by 69 nucleotides (40). The predominant, larger isoform apparently results from an alternative splice site that is about 69 nucleotides 5' of the exon 3 splice acceptor site, resulting in an ESX containing an extra 69 nucleotides in exon 3 (40). The ESX protein derived from the larger ESX mRNA encodes for a protein of 371 amino acids that is predicted to migrate at 41.4 kDa (40). In contrast, the smaller

mRNA, devoid of the 69 nucleotides, is predicted to migrate at 39.3 kDa (40). Here, we used the larger isoform of human ESX and showed that in vitro transcription-translation of this ESX cDNA in a reticulocyte lysate system produced a protein migrating at 47 kDa on SDS-PAGE gels (Fig. 2). Similarly, Western blot analysis of an HA epitope-tagged ESX expressed in HeLa cells by transient transfection also verified ESX protein as migrating at ~47 kDa (Fig. 4). Moreover, recombinant GST-ESX migrated at ~74 kDa, and allowing for the 27 kDa of GST reveals that bacterially-expressed ESX also migrates at 47 kDa (data not shown). These data contrast with those of Chang et al (50), who used a polyclonal antibody to the carboxy-terminal end of ESX to demonstrate that endogenous ESX expressed in several breast cancer cell lines (ZR75-1, MDA-468 & MDA-231) migrated as a 42 kDa protein band. Of note, this latter report did not show protein size standards, and instead only showed the ESX bands in isolation (50). These minor differences in ESX protein migration might be due to slight experimental differences.

Differential transcription potency of ESX on various Ets-target promoters

In this report, we show that ESX differentially activates various promoters, each of which contains a functional Ets binding site (EBS). Thus, ESX efficiently activated the 8Xpal, collagenase and Her2/neu promoters, but failed to activate the stromelysin promoter (Figs. 5-7). Of note, the single EBS within the stromelysin promoter is the same as the EBS that is multimerized as 8 copies in the 8xpal promoter (ATTTGGATGGAAGCAATTAT), yet ESX failed to activate the former but

clearly activated the latter. These data show that a single EBS of the type contained within the stromelysin promoter is insufficient to mediate ESX activity. By contrast, the single EBS contained within the collagenase or Her2/neu promoters appears to be sufficient to allow ESX-mediated promoter activation. The EBS within the collagenase promoter is ACTAGGAAGTGGAAA at position -85 (53) and the EBS within the Her2/neu promoter is TGCTTGAGGAAGTATAA located at position –26 (8). In addition, Choi et al (39), examined the ability of various Ets binding sites contained in 7 different promoters, including TGFß RII, Tra, IL-2Ra, PEA3, HTLV-1, CD18 and HIV2, to bind ESX by gel shift analysis, and to be activated by ESX in transient co-transfection assays. These studies identified the PEA3 (CGAGCAGGAAATGGG), TRα (AGCCACATCCTGTGGAA), TGFß RII (GGAAACAGGAAACTCCT) and HTLV-1 (CATGGGGAGGAAATGGG) Ets binding sites as binding to ESX in gel shifts studies, and as being activated 2-4-fold by co-transfected ESX (39). In a separate study, the relative binding affinity of ESX for Ets binding sites derived from 10 different epidermis-selective genes was performed and, using the resultant data, a consensus ESX binding sequence was defined as: 5'-(A/G/T)N(C/G/a)(A/c)GGA(A/t)(G/a)(T/a/c)(A/G/c)(N/t)-3' (54). While the ESX binding site sequence prefers the nucleotide A immediately upstream of the core GGA and most other Ets factors prefer a C at that site (2); nevertheless, the ESX site is quite degenerate. In this regard, a comparison of the Ets binding sites noted above for stromelysin, collagenase and Her2/neu show that the sites from the latter two ESX-stimulated genes match the consensus ESX sequence,

whereas the nonresponsive stomelysin site contains a T just upstream of the core GGA and a C three bases downstream of the core sequence. It is likely that these two changes account for the reduced ability of ESX to stimulate the stromelysin promoter. However, if this stromelysin site is present in multiple copies, as in 8Xpal, then the effects of these two nonconsensus bases are overcome.

Differential activation of the HER2/neu promoter by ten distinct Ets constructs

As noted above, the HER2/neu promoter has been shown to contain a critical EBS at position -26 (37). The Ets factors PEA3 and ESX have been shown to be overexpresssed in Her2/neu positive breast cancer cells, and to bind to the -26 site and to activate Her2/neu promoter-reporter constructs in co-transfection assays (8, 22). However, the identity of the endogenous Ets factor that actually regulates Her2/neu promoter activity via the -26 site in vivo remains unknown. Here we show that, in fact, several Ets factors stimulated the Her2/neu promoter (Fig. 7). Of note, several Ets factors have been shown to be expressed in mammary cells, including members of the PEA3 subfamily (PEA3, ER81 and ERM), GABP, Ets-1, Ets-2, ESX and Elk (55) and of these Eta factors, both PEA3 and ESX have been reported to activate the Her2/neu proximal promoter in co-transfection assays (8, 22, 37, 51). In this study, three patterns of Her2/neu promoter activation by Ets factors were demonstrated: (1) no effect or repressed promoter activity (Elk-1 and NET); (2) intermediate activity (ER81, GABP, ESX and HA-Ets-2); and, (3) maximal activity (Ets-1, VP-16-Ets-1, EHF,

and HA-VP16-ESX). This result shows that indeed multiple Ets factors, including ER81, GABP, Ets-1, Ets-2, EHF and ESX, are capable of trans-activating the Her2/neu promoter. It is noteworthy that heregulin has been shown to induce PEA3 and ESX expression, which in turn can activate the Her2/neu promoter, suggesting that a positive feedback loop between Her2/neu and specific Ets factors may exist in Her2/neu positive breast cancer cells (20, 22).

ESX and Ets-2 transform MCF-12A cells, whereas anti-sense and dominant-negative ESX inhibit T47D cell growth

The proto-oncogenes *c-Ets-1* and *c-Ets-2* are able to transform NIH 3T3 cells, but at a much reduced efficiency (less than 50-fold) compared to the *gag-myb-ets* oncogene (26). Foos et al (35) have reported that the role of Ets-2 in cellular transformation may be quite complex, since over-expression of full length Ets-2, a VP16-Ets-2 fusion or the Ets-2 DBD, reversed the Ras-mediated transformation of NIH 3T3 cells (35). By contrast, the Ets-2 TAD failed to fully reverse the transformed phenotype (35). Taken together, these data would suggest that Ets-1 and Ets-2 are weak transforming agents, and that their mechanisms of transformation may be complex.

As noted in the Introduction, the use of dominant-negative Ets-2, which encodes for only the Ets-2 DBD, has provided the most substantial data implicating Ets proteins in mammary tumorigenesis (28, 29). Specifically, dn-Ets-2 has been shown to totally block the anchorage-

independent growth and cellular invasiveness of NmuMG, MMT and BT20 breast carcinoma cells (28, 29). Moreover, the size of mammary tumors induced by a polyoma virus middle T antigen (PyMT) transgene were reduced in half in mice that were also heterozygous for a *c-Ets-2* loss-of-function mutation (56). Ets-2 may contribute to malignant transformation by inhibiting apoptosis, since Sevilla et al (13) have reported that over-expression of Ets-2 inhibits apoptosis in BAC1.2F5 macrophage cells by up-regulating Bcl-x_L. Despite these advances, the ability of Ets factors to transform mammary cells in culture has not been reported. Here we show by two separate approaches, induction of foci formation in nontransformed MCF-12A human mammary cells and inhibition of foci formation in transformed T47D cells, that Ets factors contribute to the transformed phenotype in mammary cells. Specifically, we show that HA-ESX, HA-VP16-ESX and HA-Ets-2 are each capable of inducing foci formation in MCF-12A cells, and that they do so with an efficiency approximating oncogenic V12Ras (Fig. 8). Conversely, anti-sense and dominant-negative HA-ESX constructs significantly reduced T47D foci formation (Fig. 9 and Table 2). Of note, however, ESX over-expression in the Hs578t human breast cancer cell line was shown to have a complex effect on cellular proliferation and tumorigenesis (39). In this cell line, ESX had no direct effect on cell proliferation, however ESX apparently induced an inhibitory response to added TGF-ß1 ligand and mediated a reduction in tumor size in nude mice (39). This effect was most likely due to the restoration of TGFß-II receptor expression and TGFß1 response by ESX (39). These results parallel those with PEA3, in that PEA3 has been shown to both promote and inhibit

tumorigenesis in different mammary model systems, suggesting that either the level of Ets factor expressed or the recipient cell line used confers the specificity of response. Nevertheless, these data presented here show for the first time that Ets factors, specifically ESX and Ets-2, can mediate breast cell transformation.

References

1. Wasylyk, B., Hagman, J., and Gutierrez-Hartmann, A. Ets transcription factors: nuclear effectors of the Ras/MAP kinase signaling pathway. Trends Biochem. Sci. *23:* 213-216, 1998.

2. Graves, B. and Petersen, J. Specificity within the *ets* family of transcripition factors. *In:* G. Vande Woude and G. Klein (eds.), Advances in Cancer Research, 1998.

3. Bradford, A. and Gutierrez-Hartmann, A. Ets transcription factors: Nuclear integrators of signaling pathways in the regulation of endocrine gene expression. *In:* M. Shupnick (ed.) Gene Engineering and Molecular Models in Endocrinology, pp. In press. Totowa, NY: Humana Press, Inc., 1998.

4. Dittmer, J. and Nordheim, A. Ets transcription factors and human disease., Bioch. Biophys. Acta. *1377:* F1-F11, 1998.

5. Donaldson, L., Petersen, J., Graves, B., and McIntosh, L. Secondary structure of the ETS domain places murine Ets-1 in the superfamily of winged helix-turn-helix DNA-binding proteins., Biochemistry. *33:* 13509-13516, 1994.

6. Donaldson, L., Petersen, J., Graves, B., and McIntosh, L. Solution structure of the ETS domain from murine Ets-1: A winged helix-turn-helix DNA-binding motif., EMBO J. *15:* 125-134, 1996.

7. Leprince, D., Gegonne, A., Coll, J., deTaisne, D., Schneeberger, A., Largrou, C., and Stehelin, D. A putative second cell-derived oncogene of the avian leukemia retrovirus E26, Nature. *306:* 395-397, 1983.

8. Scott, G., Daniel, J., Xiong, X., Maki, R., Kabat, D., and Benz, C. Binding of an Ets-related protein within the DNase I hypersensitive site of the HER2/neu promoter in human breast cancer cells, J. Biol. Chem. *269:* 19848-19858, 1994.

9. Oda, N., Abe, M., and Sato, Y. ETS-1 converts endothelial cells to the angiogenic phenotype by inducing the expression of matrix metalloproteinases and integrin beta3., J. Cell. Physiol. *178:* 121-132, 1999.

10. Takaoka, A., Yamada, T., Gotoh, M., Kanai, Y., Imai, K., and Hirohashi, S. Cloning and characterization of the human beta4-integrin gene promoter and enhancers., J. Biol. Chem. *273:* 33848-33855, 1998.

11. Rodrigo, I., Cato, A., and Cano, A. Regulation of E-cadherin gene expression during tumor progression: The role of a new Ets-binding site and the E-pal element., Exp. Cell. res.. *248:* 358-371, 1999.

12. Gilles, C., Polette, M., Birembaut, P., Brunner, N., and Thompson, E. Expression of c-ets-1 mRNA is associated with invasive, EMT-derived phenotype in breast carcinoma cell lines., Clin. Exp. Metastasis. *15:* 519-526, 1997.

13. Sevilla, L., Aperlo, C., Dulic, V., Chambard, J., Boutonnet, C., Pasquier, O., Pognonec, P., and Boulukos, K. The Ets2 transcription factor inhibits apoptosis induced by colony-stimulating factor-1 deprivation of macrophages through a Bcl-x_L-dependent mechanism., Mol. Cell. Biol. *19:* 2624-2634, 1999.

14. Albanese, C., Johnson, J., Watanabe, G., Eklund, N., Vu, D., Arnold, A., and Pestell, R. Transforming p21ras mutants and c-Ets-2 activate the cyclin D1 promoter through distinguishable regions., J. Biol. Chem. *270:* 23589-23597, 1995.

15. Tetsu, O. and McCormick, F. Beta-catenin regulates expression of cyclin D1 in colon carcinoma cells., Nature. *398:* 422-426, 1999.

16. Treisman, R. The serum response element, Trends Biochem. Sci. *17:* 423-426, 1992.

17. Roussel, M., Davis, J., Cleveland, J., Ghysdael, J., and Hiebert, S. Dual control of myc expression through a single DNA binding site targeted by ets family proteins and E2F-1., Oncogene. *9:* 405-415, 1994.

18. Wasylyk, B. and Nordheim, A. Ets transcription factors: Partners in the integration of signal responses. *In:* A. Papavassiliou (ed.) Transcription Factors in Eukaryotes, pp. 251-284: Landes Bioscience, 1997.

19. O'Hagan, R. and JA, H. The PEA3 Ets transcription factor is a downstream target of the HER2/Neu receptor tyrosine kinase., Oncogene. *16:* 301-310, 1998.

20. Neve, R., Chang, C.-H., Scott, G., Wong, A., Friis, R., Hynes, N., and Benz, C. The epithelium-specific Ets transcription factor ESX is associated with mammary gland development and involution., FASEB J. *12:* 1541-1550, 1998.

21. Baert, J., Monte, D., Musgrove, E., Albagli, O., Sutherland, R., and Delaunoit, Y. Expression of the PEA3 group of Ets-related transcription factors in human breast cancer cells, Int. J. Cancer. *70:* 590-597, 1997.

22. Benz, C., O'Hagan, R., Richter, B., Scott, G., Chang, C.-H., Xiong, X., Chew, K., Ljung, B.-M., Edgerton, S., Thor, A., and Hassell, J. HER2/Neu and the Ets transcription activator PEA3 are coordinatley upregulated in human breast cancer., Oncogene. *15:* 1513-1525, 1997.

23. Watabe, T., Yoshida, K., Shindoh, M., Kaya, M., Fujikawa, K., Sato, H., Seiki, M., Ishii, S., and Fujinaga, K. The Ets-1 and Ets-2 transcription factors activate the promoters for invasion-associated urokinase and collagenase genes in response to epidermal growth factor., Int. J. Cancer. *77:* 128-137, 1998.

24. Zhang, M., Maass, N., Magit, D., and Sager, R. Transactivation through Ets and AP1 transcription sites determines the expression of the tumor-supressing gene maspin., Cell Growth Diff. *8:* 179-186, 1997.

25. Robinson, L., Panayiotakis, A., Papa, T., Kola, I., and Seth, A. ETS target genes: Identification of egr1 as a target by RNA differential display and whole genome techniques., Proc. Natl. Acad. Sci. USA. *94:* 7170-7175, 1997.

26. Seth, A. and Papa, T. The c-ets-1 proto-oncogene has oncogenic activity and is positively autoregulated., Oncogene. *5:* 1761-1767, 1990.

27. Galang, C., Der, C., and Hauser, C. Oncogenic Ras can induce transcriptional activation through a variety of promoter elements, including tandem c-Ets-2 binding sites, Oncogene. *9:* 2913-2921, 1994.

28. Sapi, E., Flick, M., Rodov, S., and Kacinski, B. Ets-2 transdominant mutant abolishes anchorage-independnet growth and amcropahge-stimulating factor-stimulated invasion by BT20 breast carcinoma cells., Cancer Res. *58:* 1027-1033, 1998.

29. Delannoy-Courdent, A., Mattot, V., Fafeur, V., Fauquette, W., Pollet, I., Calmels, T., Vercamer, C., Boilly, B., Vandenbunder, B., and Desbiens, X. The expression of Ets-1 transcription factor lacking its activation domain decreases uPA proteolytic activity and cell motility, and impairs normal tubulogenesis and cancerous scattering in mammary epithelial cells., J. Cell Sci. *111:* 1521-1534, 1998.

30. Wasylyk, C., Maira, S.-M., Sobieszczuk, P., and Wasylyk, B. Reversion of Ras transformed cells by Ets transdominant mutants, Oncogene. *9:* 3665-3673, 1994.

31. Langer, S. J., Bortner, D. M., Roussel, M. F., Sherr, C. J., and Ostrowski, M. C. Mitogenic signaling by colony-stimulating factor 1 and *ras* is suppressed by the *ets*-2 DNA-binding domain and restored by *myc* overexpression., Mol. Cell. Biol. *12:* 5355-5362, 1992.

32. Bradford, A. P., Conrad, K. E., Wasylyk, C., Wasylyk, B., and Gutierrez-Hartmann, A. Functional interaction of c-Ets-1 and GHF-1/Pit-1 mediates Ras activation of pituitary-specific gene expression: Mapping of the essential c-Ets-1 domain, Mol. Cell. Biol. *15:* 2849-2857, 1995.

33. Bradford, A., Conrad, K., Tran, P., Ostrowski, M., and Gutierrrez-Hartmann, A. GHF-1/Pit-1 functions as a cell specific integrator of Ras signalling by targeting the Ras pathway to a composite Ets-1/GHF-1 response element, J. Biol. Chem. *271:* 24639-24648, 1996.

34. Bradford, A., Wasylyk, C., Wasylyk, B., and Gutierrez-Hartmann, A. Interaction of Ets-1 and the POU-homeodomain GHF-1/Pit-1 reconstitutes pituitary specific gene expression., Mol. Cell. Biol. *17:* 1065-1074, 1997.

35. Foos, G., Garcia-Ramirez, J., Galang, C., and Hauser, C. Elevated expression of Ets2 or distinct portion of Ets2 can reverse Ras-mediated cellular transformation., J. Biol. Chem. *273:* 18871-18880, 1998.

36. Galang, C., Garcia-Ramirez, J., Solski, P., Westwick, J., Der, C., Neznanov, N., Oshima, R., and Hauser, C. Oncogenic Neu/ErbB-2 increases, Ets, AP-1 and NF-kB-dependent gene expression, and inhibiting Ets activation blocks Neu-mediated cellular transformation, J. Biol. Chem. *271:* 7992-7998, 1996.

37. Chang, C., Scott, G., Kuo, W., Xiong, X., Suzdaltseva, Y., Park, J., Sayre, P., Erny, K., Collins, C., Gray, J., and Benz, C. ESX: A structurally unique Ets overexpressed early during human breast tumorigenesis, Oncogene. *14:* 1617-1622, 1997.

38. Andreoli, J., Jang, S.-I., Chung, E., Coticchia, C., Steinert, P., and Markova, N. The expression of a novel, epithelium-specific ets transcription factor is restricted to the most differentiated layers in the epidermis, Nucleic Acids Research. *25:* 4287-4295, 1997.

39. Choi, S.-G., Yi, Y., Kim, Y.-S., Kato, M., Chang, J., Chung, H.-W., Hahm, K.-B., Yang, H.-K., Rhee, H., Bang, Y.-J., and Kim, S.-J. A novel Ets-related transcription factor, ERT/ESX/ESE-1, regulates expression of the transforming growth factor-ß type II receptor., J. Biol. Chem. *273:* 110-117, 1998.

40. Oettgen, P., Alani, R., Barcinski, M., Brown, L., Akbarali, Y., Boltax, J., Kunsch, C., Munger, K., and Libermann, T. Isolation and characterization of a novel epithelium-specific transcription factor, ESE-1, a member of the *ets* family., Mol. Cell. Biol. *17:* 4419-4433, 1997.

41. Tymms, M., Ng, A., Thomas, R., Schutte, B., Zhou, J., eyre, H., Sutherland, G., Seth, A., Rosenberg, M., Papas, T., Debouck, C., and Kola, I. A novel epithelial-expressed ETS gene, ELF3: Human and murine cDNA sequences, murine genomic organization, human mapping to 1q.32.2 and expression in tissues and cancer., Oncogene. *15:* 2449-2462, 1997.

42. Oettgen, P., Barcinski, M., Boltax, J., Stolt, P., Akbarali, Y., and Libermann, T. Genomic organization of the human ELF3 (ESE-1/ESX) gene, a member of the Ets transcription factor family, and identification of a functional promoter., Genomics. *55:* 358-362, 1999.

43. Liu, E., Thor, A., He, M., Barcos, M., Ljung, B., and Benz, C. The HER2 (c-erbB-2) oncogene is frequently amplified in *in situ* carcinomas of the breast., Oncogene. *7:* 1027-1032, 1992.

44. Bradford, A. P., Brodsky, K. S., Diamond, S. E., Kuhn, L. C., Liu, Y., and Gutierrez-Hartmann, A. The Pit-1 homeodomain and ß-domain interact with Ets-1 and modulate synergistic activation of the rat prolactin promoter., J. Biol. Chem. *275:* 3100-3106, 2000.

45. Gordon, D., Lewis, S., Haugen, B., James, R., McDermott, M., Wood, W., and Ridgway, E. Pit-1 and GATA-2 interact and functionally cooperate to activate the thyrotropin ß-subunit promoter., J. Biol. Chem. *272:* 24339-24347, 1997.

46. Tanaka, M. and Herr, W. Reconstitution of transcriptional activation domains by reiteration of short peptide segments reveals the modular organization of a glutamine-rich activation domain., Mol. Cell. Biol. *14:* 6056-6067, 1994.

47. Wasylyk, C., Gutman, A., Nicholson, R., and Wasylyk, B. The c-Ets oncoprotein activates the stromelysin promoter through the same elements as several non-nuclear oncoproteins., EMBO J. *10:* 1127-1134, 1991.

48. Angel, P., Imagawa, M., Chiu, R., Stein, B., Imbra, R. J., Rahmsdorf, H. J., Jonat, C., Herrlich, P., and Karin, M. Phorbol ester-inducible genes contain a common *cis* element recognized by a TPA-modulated trans-acting factor, Cell. *49:* 729-739, 1987.

49. Maxwell, I. H., Harrison, G. S., Wood, W. M., and Maxwell, F. A DNA cassette containing a trimerized SV40 polyadenylation signal which efficiently blocks spurious plasmid-initiated transcription, Biotechniques. *7:* 276-280, 1989.

50. Chang, C.-H., Scott, G. K., Baldwin, N. A., and Benz, C. C. Exon 4-encoded acidic domain in the epithelium-restricted Ets factor, ESX, confers potent transactivating capacity and binds to TATA-binding protein (TBP)., Oncogene. *18:* 3682-95, 1999.

51. Xing, X., Wang, S. C., Xia, W., Zou, Y., Shao, R., Kwong, K. Y., Yu, Z., Zhang, S., Miller, S., Huang, L., and Hung, M. C. The Ets protein PEA3 suppresses Her-2/neu overexpression and inhibits tumorigenesis., Nat. Medicine. *6:* 189-195, 2000.

52. Trimble, M. S., Xin, J. H., Guy, C. T., Muller, W. J., and Hassell, J. A. PEA3 is overexpressed in mouse metastatic mammary adenocarcinomas., Oncogene. *8:* 3037-3042, 1993.

53. Pendas, M., Balbin, M., Llano, E., Jimenez, M., and Lopez-Otin, C. Structural Analysis and Promoter Characterization of the Human Collagenase-3 Gene (MMP13), Genomics. *40:* 222-233, 1997.

54. Oettgen, P., Kas, K., Dube, A., Gu, X., Grall, F., Thamrongsak, U., Akbarali, Y., Finger, E., Boltax, J., Endress, G., Munger, K., Kunsch, C., and Liebermann, T. A. Characterization of ESE-2, a novel ESE-1-related Ets transcription factor that is restricted to glandular epithelium and differentiated keratinocytes., J. Biol. Chem. *274:* 29439-29452, 1999.

55. Shepherd, T. and Hassell, J. Role of Ets transcription factors in mammary gland development and oncogenesis., J. Mammary Gland Biology & Neoplasia. *6:* In press., 2000.

56. Neznanov, N., Man, A., Yamamoto, H., Hauser, C., Cardiff, R., and Oshima, R. A Single Targeted Ets2 Allele Restricts Development of Mammary Tumors in Transgenic Mice, Cancer Research. *59:* 4242-4246, 1999.

Table 1

Foci induction in MCF-12A cells by Ets factors[+]

Empty Vector	HA-ESX	HA-VP16-ESX	HA-Ets-2	V12-Ras
6 (±3)	17 (±6)	20 (±5)	23 (±17)	32 (±8)

[+]Triplicate results shown in Fig. 8B were counted (colonies ≥ 1 mm) and the average number of foci per plate (± S.D.) are tabulated.

Table 2

Inhibition of T47D foci formation by inhibitory ESX constructs[+]

% FCS	**HA-antisense-ESX**	**HA-ESX DBD**	**Empty Vector**
0.1	67 (22%)*	52 (17%)	303
1	82 (28%)	67 (22%)	301
5	126 (39%)	146 (45%)	326

[+]Triplicate results shown in Fig 9 were counted and the average number of foci per plate is tabulated.

*Numbers in paranthesis represent the % of total foci formed by empty vector.

Figure Legends

Fig. 1 Primary structure of normal and tagged human ESX protein. (A) Schematic structure of ESX protein. ESX coding sequence includes an amino (N) terminal pointed domain (pointed), the serine box (SER), an A/T hook region, and a carboxy-terminal (C) ETS DNA binding domain (DBD). **(B)** HA-tagged human ESX. Cloning results in an amino terminally HA tagged ESX. **(C)** HA-VP16-ESX construct includes the VP16 transactivation domain of herpes virus fused directly onto the amino end of ESX in the pCGN2-HA vector.

Fig. 2 In vitro transcription and translation of HA-ESX. Lanes 1 and 2 represent the in vitro transcription and translation reaction with no input DNA. One μg of chicken Ets-1 was used as a positive control (lanes 3 and 4) and 1 μg of pCDNA3.1-ESX was used for the in vitro transcription and translation of ESX. Radio-labeled translation products were separated by SDS-PAGE. The arrow denotes ESX protein, the size of which was determined by plotting the relative migration of ESX vs. the log molecular weight.

Fig. 3. Expression of HA-ESX and HA-VP16-ESX protein in transfected HeLa cells. HeLa cells were transiently transfected by electroporation with empty vector (lane 2), 10 μg HA-ESX (lane 3), 10 μg HA-VP16-ESX (lane 4), and positive control HA-MAPK (lane 5). HA-tagged

proteins were immunoprecipitated using a monoclonal anti-HA antibody and a Western blot was performed using a monoclonal anti-HA antibody to detect HA tagged proteins. Lane 1 shows the migration of protein size standards.

Fig. 4. Activation of the 8xpal promoter by HA-ESX, HA-VP16-ESX, HA-Ets-2 and V12-Ras. HeLa cells were co-transfected with the reporter construct 8xpal/pBLCAT and various doses of effector plasmids. pCGN2 vector was used for the vector control (lanes 1-2). Lanes 3-8 show CAT activity in response to three increasing doses of HA-ESX, 1, 2, and 4 μg respectively, (performed in duplicate). Responses to 1, 2, and 4 μg of HA-VP16-ESX are shown in lanes 9-14. Two positive controleffectors were used, including 2 μg of HA-Ets-2 (lanes 15-16) and 2 μg of V12-Ras (lanes 17-18). **(B)** Percent of total chloramphenicol that was acetylated by the activation of the 8xpal promoter in response to HA-ESX, HA-VP16-ESX, HA-Ets-2 and V12-Ras. The amount of CAT activity in percent was calculated by dividing the amount of acetylated chloramphenicol by the amount of total chloramphenicol in the duplicate samples, and the mean is shown ± SD, as described in Methods.

Fig. 5. Activation of the stromelysin promoter by V12-Ras and c-Ets-1 but not HA-ESX, HA-VP16-ESX, or HA-Ets-2. (A) HeLa cells were transfected with 5 μg of a stromelysin-CAT construct containing -1100/+8 of the rat stromelysin promoter together with 10 μg of empty vector

(lanes 1-2), HA-ESX (lanes 3-4), HA-VP16-ESX (lanes 5-6), HA-Ets-2 (lanes 7-8), V12-Ras (lanes9-10), or c-Ets-1 (lanes 11-12). **(B)** Quantitation of CAT activity produced by the -1100/+8 stromelysin-CAT construct in response to various effector plasmids. The % acetylated chloramphenicol was calculated as described in Fig.4.

Fig. 6. Activation of the collagenase promoter by HA-ESX, HA-VP16-ESX, and HA-Ets-2 in HeLa cells. **(A)** Five μg of the human collagenase promoter (-517/+63) fused to a CAT reporter gene was transfected into HeLa cells with 1, 5, or 10 μg of HA-ESX or HA-VP16-ESX. Ten μg of human HA-Ets-2 and V12-Ras served as positive controls for human collagenase promoter activity. **(B)** Quantitation of CAT activity produced by the -517 collagenase-CAT construct in response to various effector plasmids.

Fig. 7. Transcription potency of various Ets factor constructs on the human Her2/neu promoter. **(A)** The transcription effects of Elk-1, ER-81, c-Ets-1, VP16-c-Ets-1 and V12-Ras on the Human Her2/neu promoter. In a 96 well plate, doses of 10, 30, 60, and 100 ng of effector DNA were transfected into HeLa cells together with 100 ng of Her2/neu-pA3Luc reporter plasmid. Empty vector pSG5, containing the SV40 promoter, served as the negative control for these effectors, since the SV40 promoter is common to all of these constructs. **(B)** The transcription effects of NET, GABP, EHF, HA-ESX, HA-VP16-ESX, and HA-Ets-2 on the Her2/neu promoter.

In a 96 well plate, doses of 10, 30, 60, and 100 ng of effector DNA were transfected into HeLa cells together with 100 ng of Her2/neu-pA3Luc reporter plasmid. Empty vector pCGN2, containing the CMV promoter, served as the negative control for these effectors, since the CMV promoter is common to all of these constructs. Activation of reporter plasmids by the various transcription factors was determined by measuring normalized luciferase activity, which was then calculated as fold activity of the empty vector control, as detailed in Methods.

Fig. 8. Esx and Ets-2 induce foci formation of nontransformed MCF-12A breast cells. (A) Human MCF-12A mammary cells were transfected by electroporation with 10 μg of pCGN2 (empty vector), pSV-Ras (V12-Ras) or pCGN2-HA-VP16-ESX DNA (HA-VP16-ESX), and $1x10^3$ electroporated cells were plated per dish, in duplicate. Plates were incubated for 13 days and media was changed every 2-3 days throughout the 13 day incubation. Following this incubation cells were fixed and stained. **(B)** Human MCF-12A mammary cells were transfected by electroporation with 10 μg of pCGN2 (empty vector), pCGN2-HA- ESX (HA-ESX), pCGN2-HA-VP16-ESX DNA (HA-VP16-ESX), pCGN-HA-Ets-2 (HA-Ets-2), or pSV-Ras (V12-Ras), as described above, in triplicate.

Fig. 9. Antisense-ESX and HA-ESX DBD inhibit foci formation of transformed T47D breast cancer cells. T47D cells were co-transfected with a plasmid encoding green fluorescent protein

(GFP) and plasmids encoding inhibitory ESX effectors (antisense HA-ESX or dominant-negative HA-ESX DBD) or empty vector (shown at the top). Transfected cells were sorted according to green fluorescence and 2,000 sorted cells were plated in 60 mm dishes, in three different concentrations of fetal calf serum, 0.1%, 1% or 5% (shown on the left), and then allowed to incubate for 13 days. Colonies were fixed and stained.

Acknowledgments

We thank Drs. Bo Wasylyk for the 8Xpal/pBLCAT, -1100/+8 stromelysin and –517/+63 collagenase reporters, and the pTL1-Elk-1, pSG5-Ets-1, pSG5-VP16-Ets-1, and pTL2-hNet constructs; Michael Ostrowski for the pCGN-HA-Ets-2 plasmid; and Drs. Ralph Janknecht, Frank Burton and Tom Brown for the pSG5-ER81, pCDNA3.1-EHF, and pCMX-GABPα and pCMX-GABPß plasmids, respectively. We also acknowledge Drs. Dawn Duval, Andy Bradford and Twila Jackson for critical reading of this manuscript. Tissue culture media, DNA sequencing and FACS were provided by Core Facilities of the University of Colorado Comprehensive Cancer Center (NIH P30 CA 46934). JTT was supported by an NIH T32 DK074461 award and grant DOD DAMD17-97-1-7307, and SED was supported by a Postdoctoral Fellowship from the Lalor Foundation, a UCCR Seed Grant, and an NIH K01 DK02752-01 award. Boehringer Ingelheim, Austria GmbH, provided initial support for this work, and subsequent support was provided by grant DOD DAMD17-00-1-0476 to AGH.

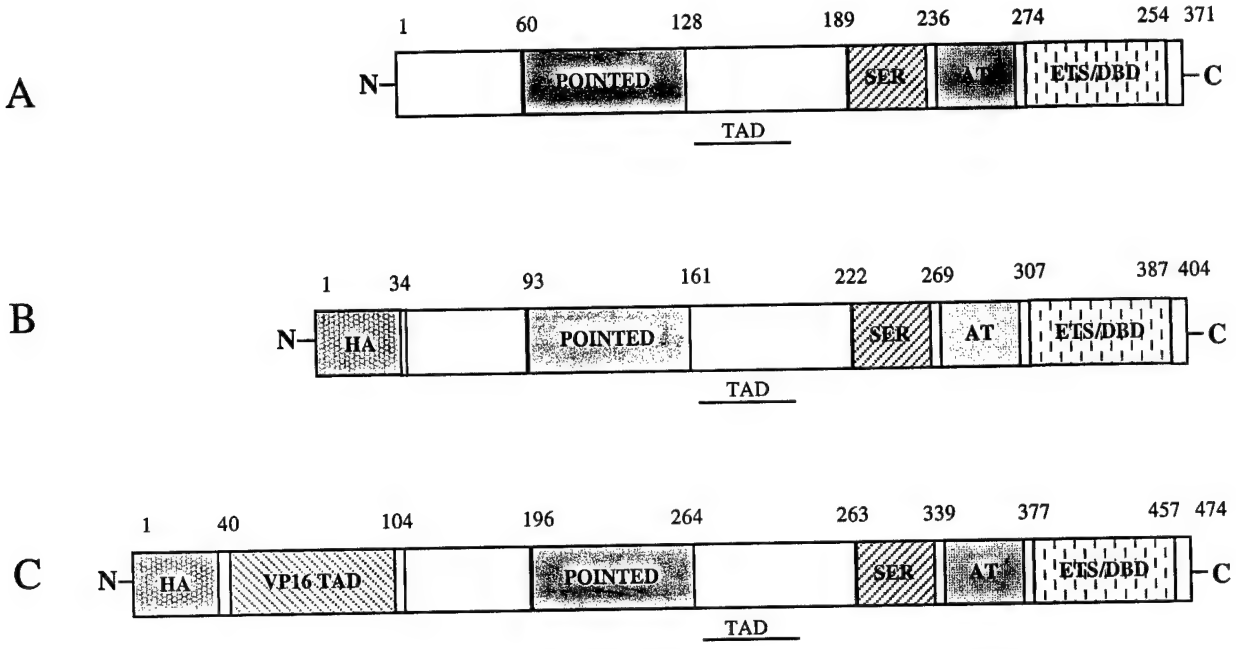
A
1
60
128
189
236
274
254
371
N
POINTED
SER
AT
ETS/DBD
C
TAD
B
1
34
93
161
222
269
307
387
404
N
HA
POINTED
SER
AT
ETS/DBD
C
TAD
C
1
40
104
196
264
263
339
377
457
474
N
HA
VP16 TAD
POINTED
SER
AT
ETS/DBD
C
TAD

Figure 1

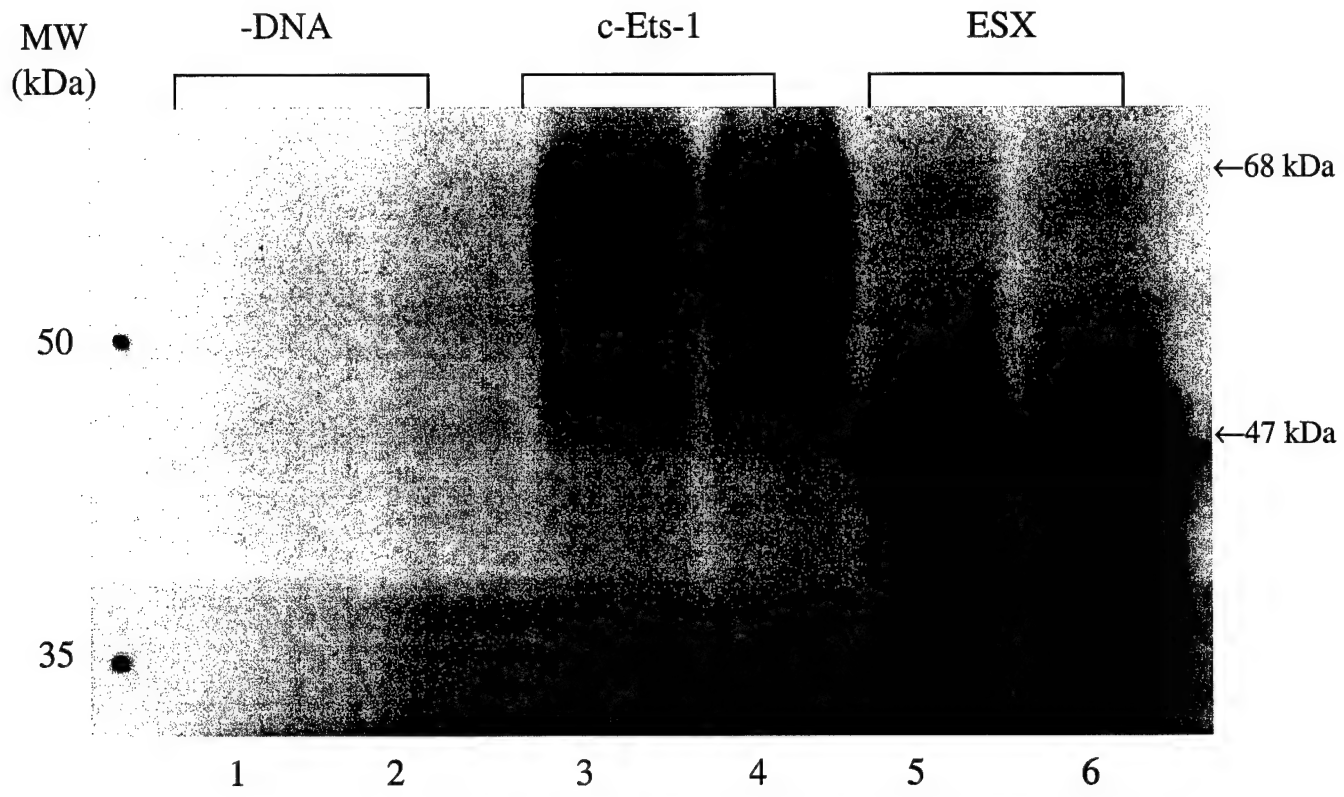

Figure 2

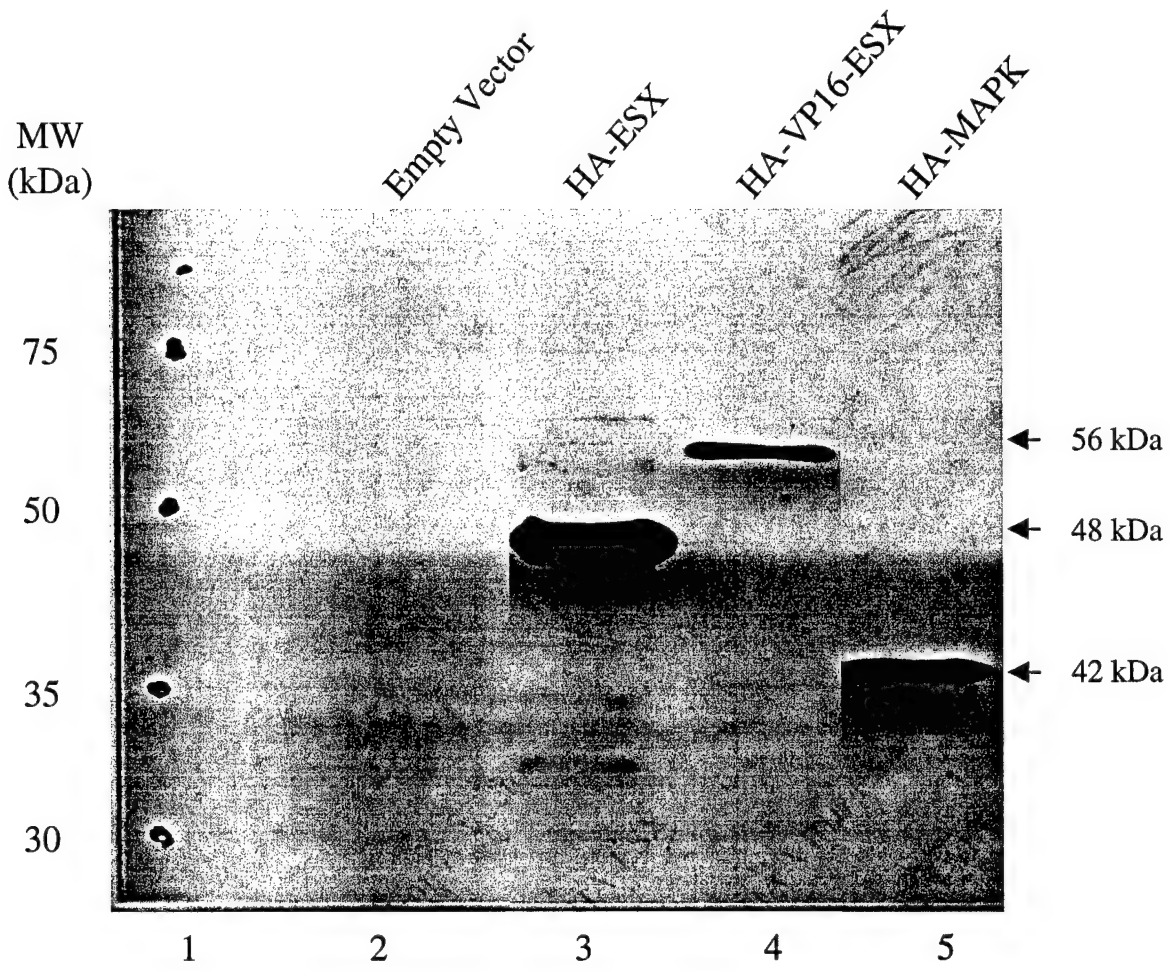
MW
(kDa)
Empty Vector
HA-ESX
HA-VP16-ESX
HA-MAPK
75
50
35
30
56 kDa
48 kDa
42 kDa
1
2
3
4
5

Figure 3

A

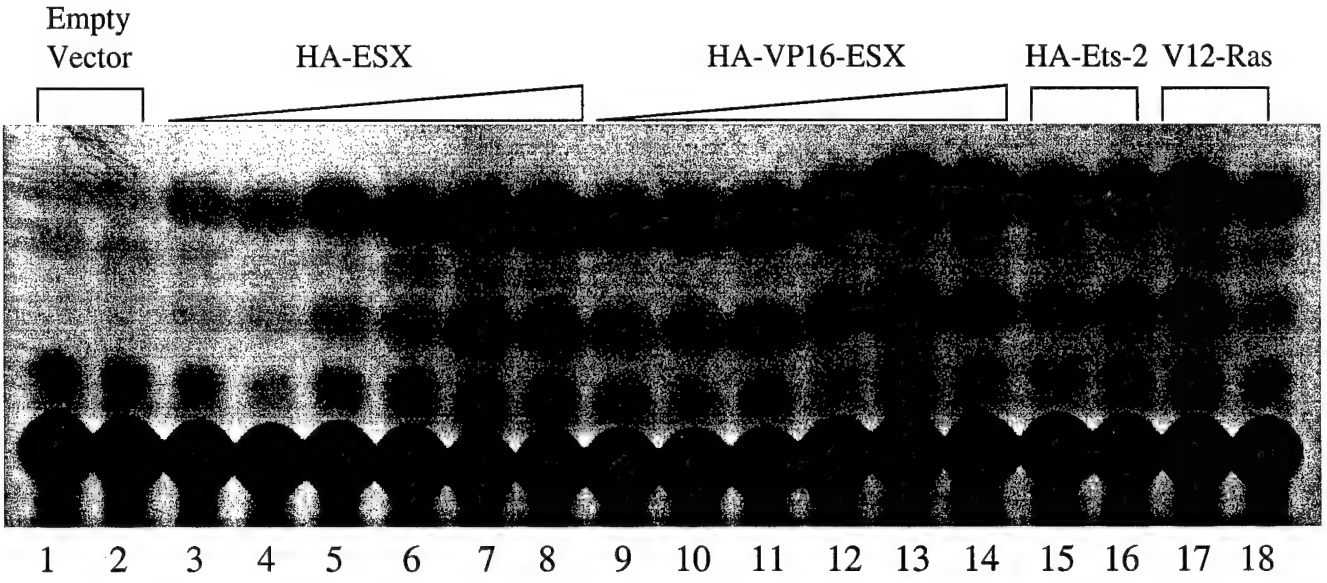
Empty Vector
HA-ESX
HA-VP16-ESX
HA-Ets-2
V12-Ras
1 2 3 4 5 6 7 8 9 10 11 12 13 14 15 16 17 18

B

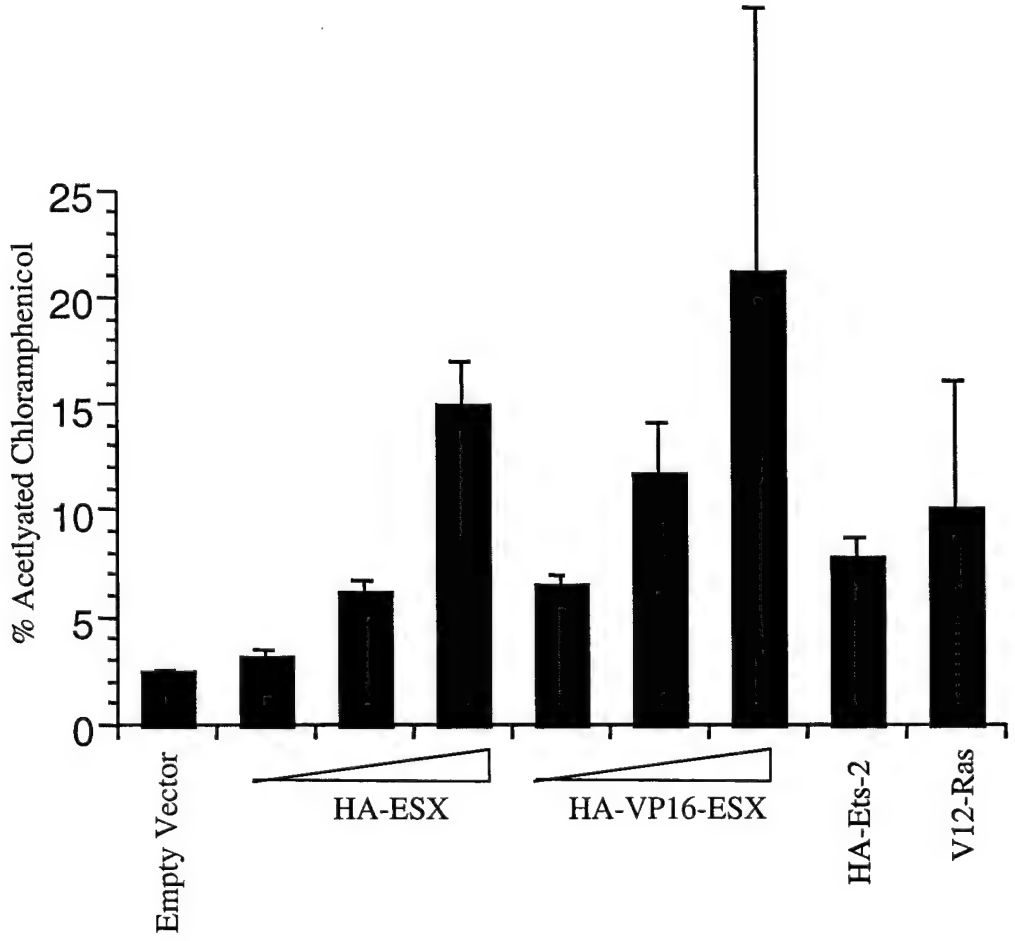
% Acetlyated Chloramphenicol
25
20
15
10
5
0
Empty Vector
HA-ESX
HA-VP16-ESX
HA-Ets-2
V12-Ras

Figure 4

A

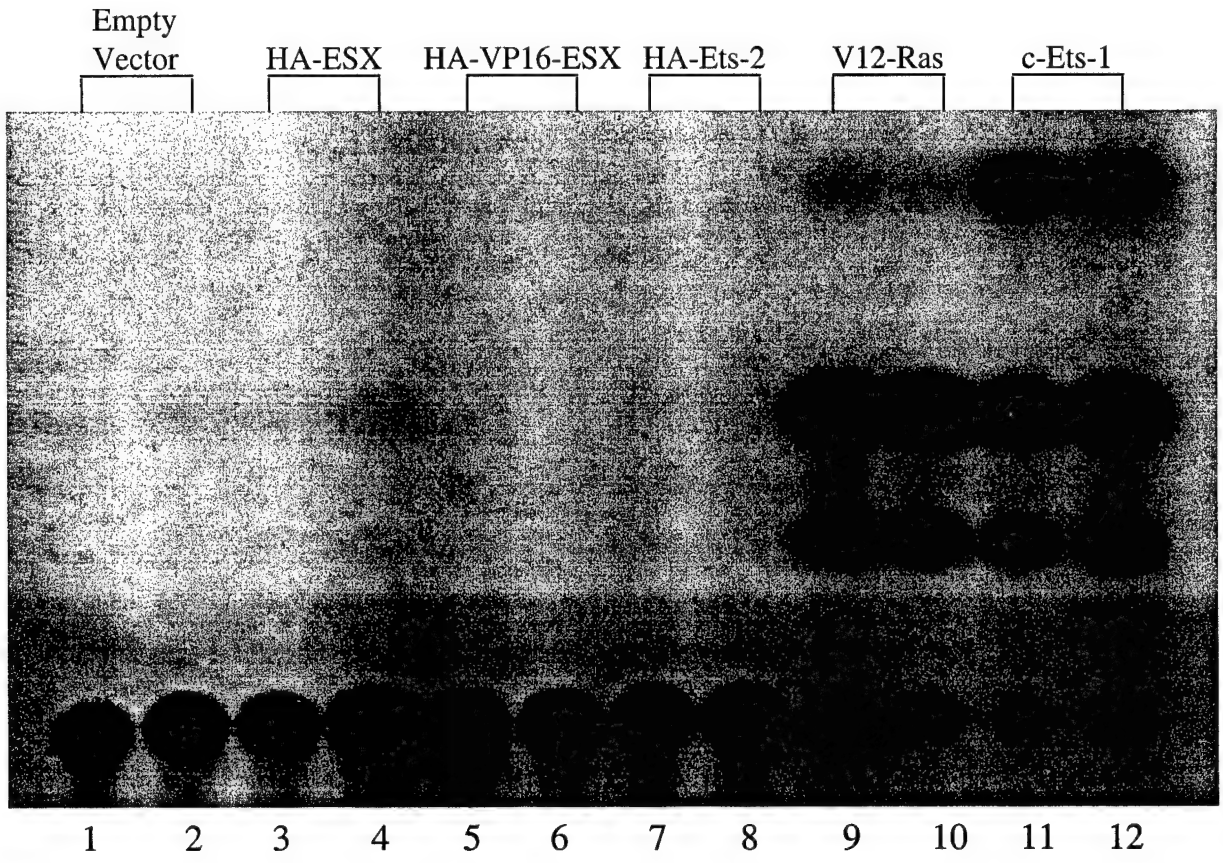
Empty Vector
HA-ESX
HA-VP16-ESX
HA-Ets-2
V12-Ras
c-Ets-1
1 2 3 4 5 6 7 8 9 10 11 12

B

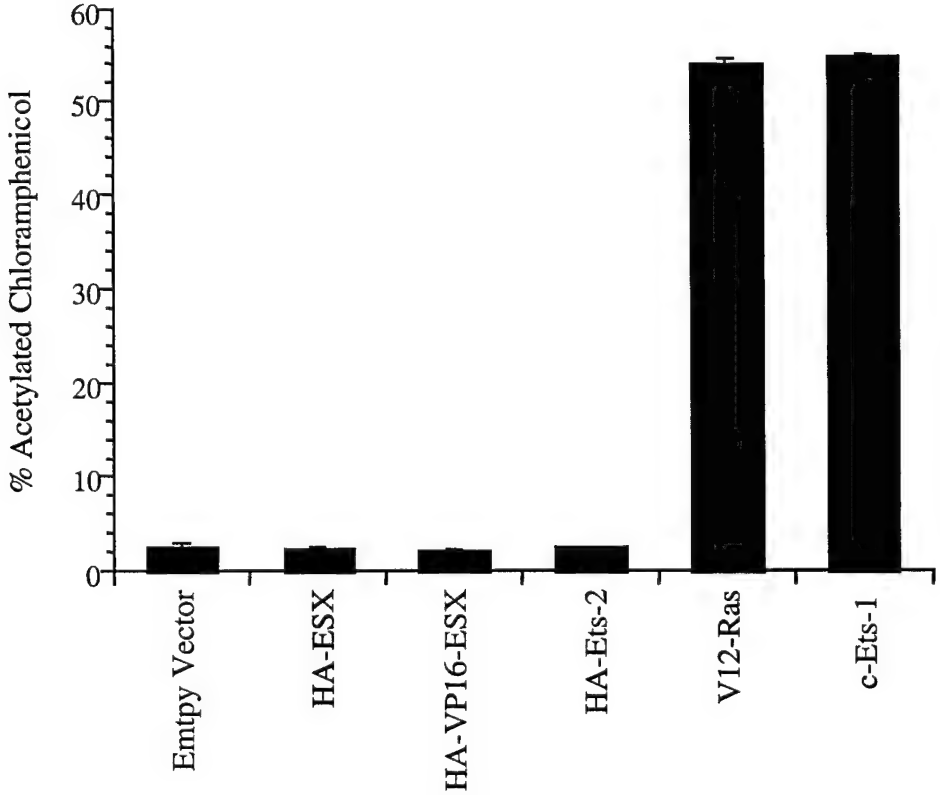
% Acetylated Chloramphenicol
60
50
40
30
20
10
0
Emtpy Vector
HA-ESX
HA-VP16-ESX
HA-Ets-2
V12-Ras
c-Ets-1

Figure 5

A

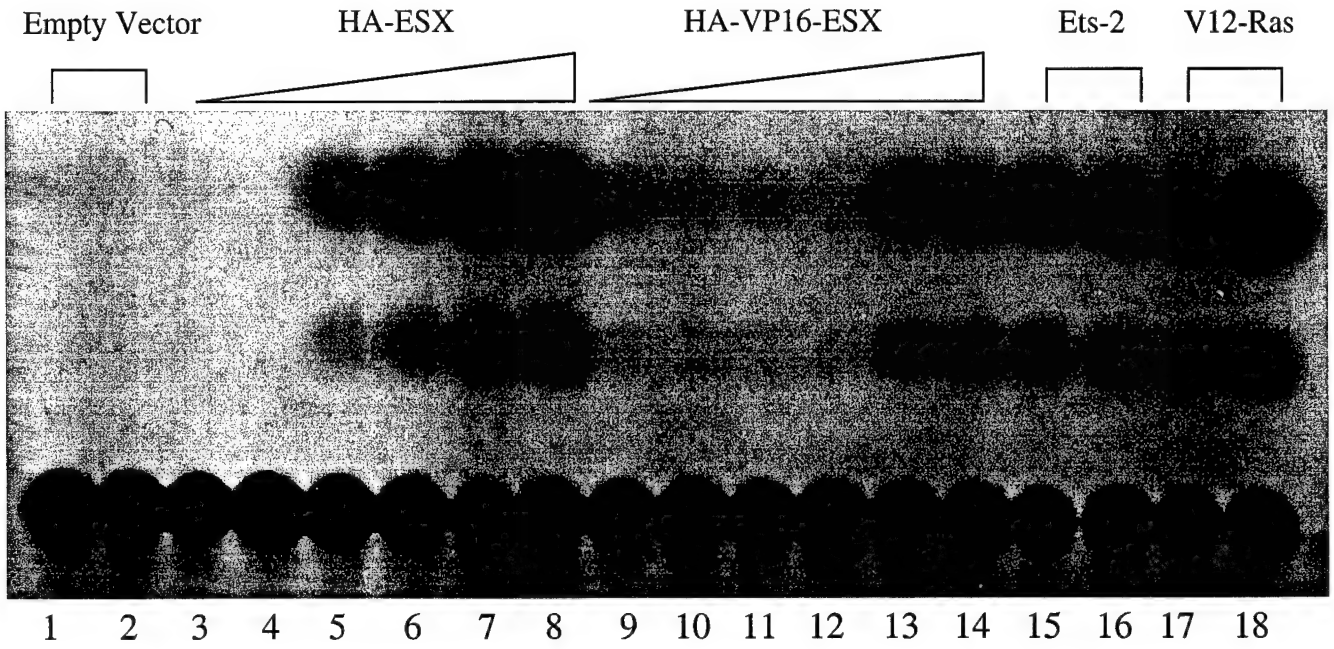
Empty Vector
HA-ESX
HA-VP16-ESX
Ets-2
V12-Ras
1 2 3 4 5 6 7 8 9 10 11 12 13 14 15 16 17 18

B

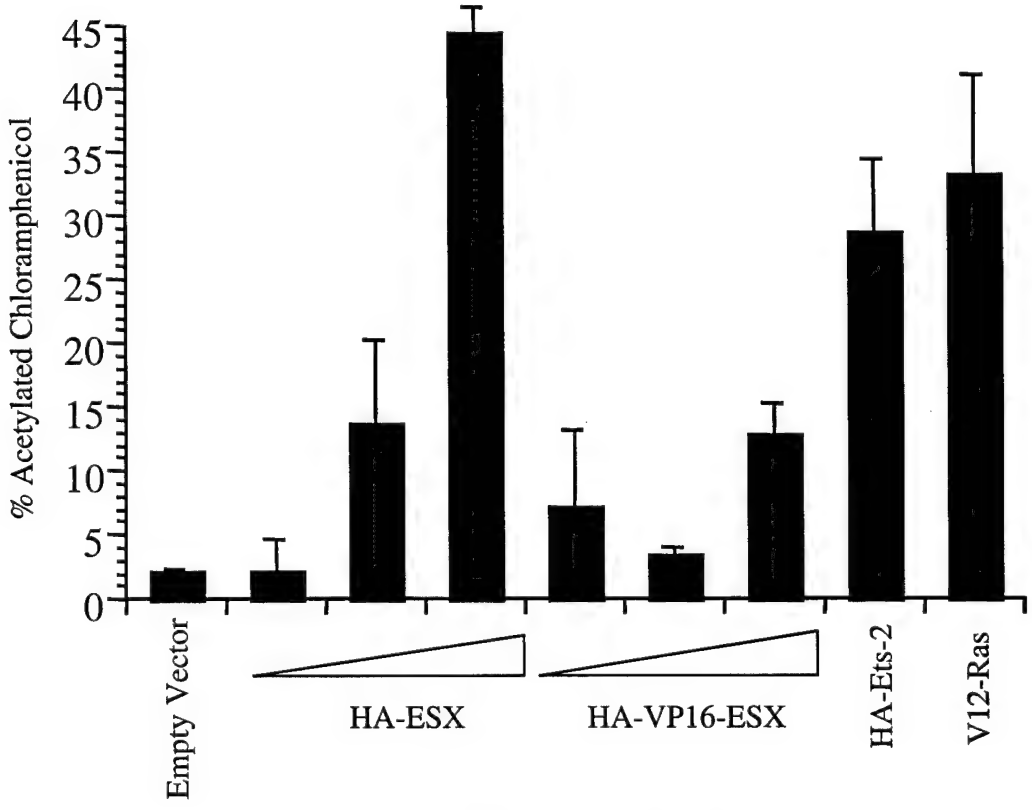
% Acetylated Chloramphenicol
0
5
10
15
20
25
30
35
40
45
Empty Vector
HA-ESX
HA-VP16-ESX
HA-Ets-2
V12-Ras

Figure 6

A

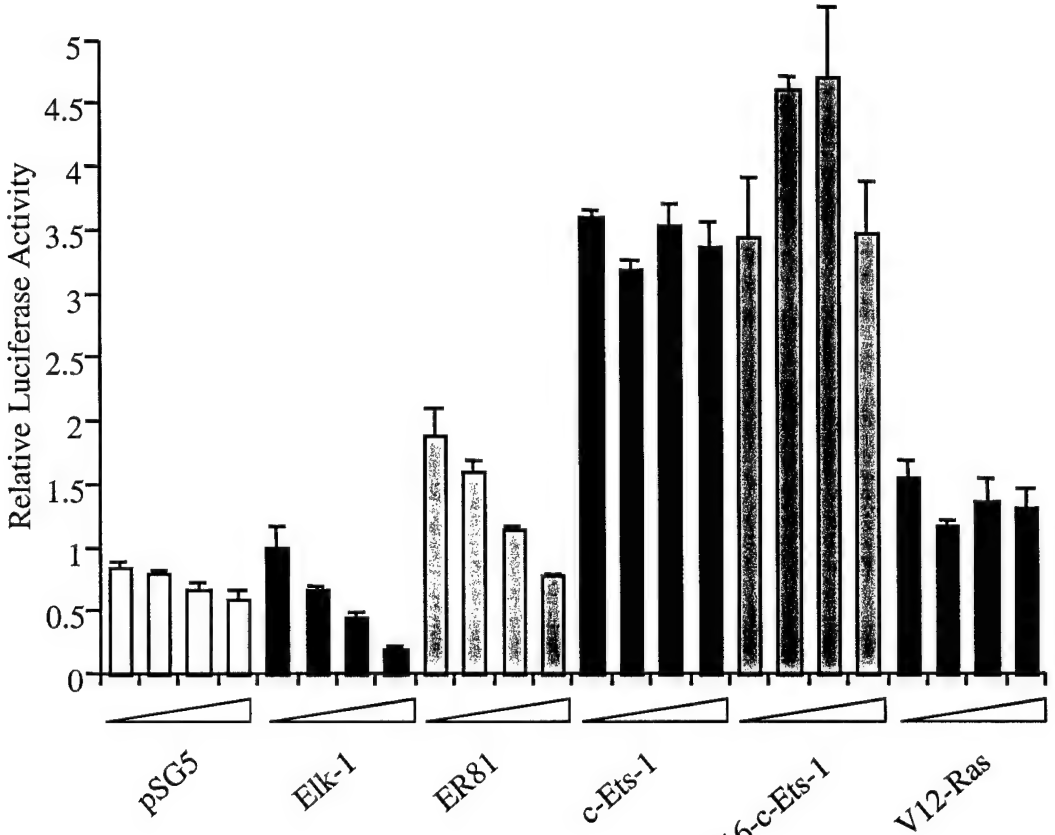
Relative Luciferase Activity
5
4.5
4
3.5
3
2.5
2
1.5
1
0.5
0
pSG5
Elk-1
ER81
c-Ets-1
VP16-c-Ets-1
V12-Ras

B

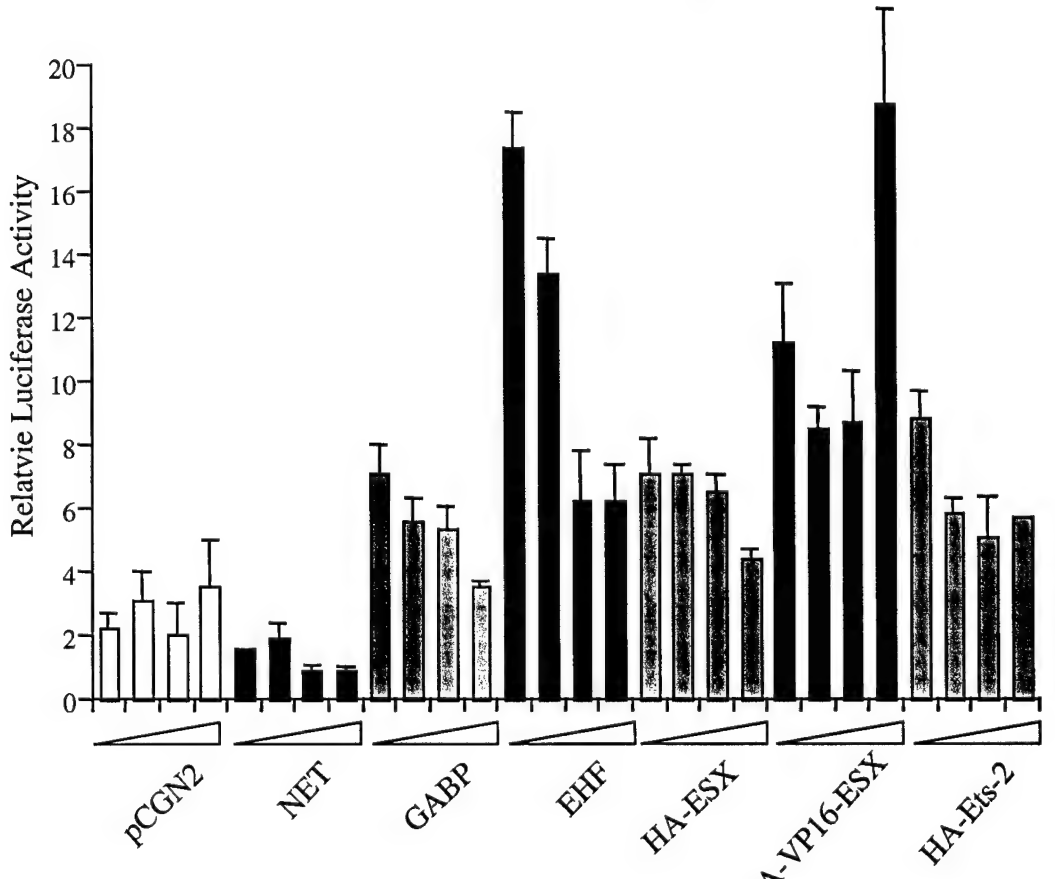
Relatvie Luciferase Activity
20
18
16
14
12
10
8
6
4
2
0
pCGN2
NET
GABP
EHF
HA-ESX
HA-VP16-ESX
HA-Ets-2

Figure 7

A

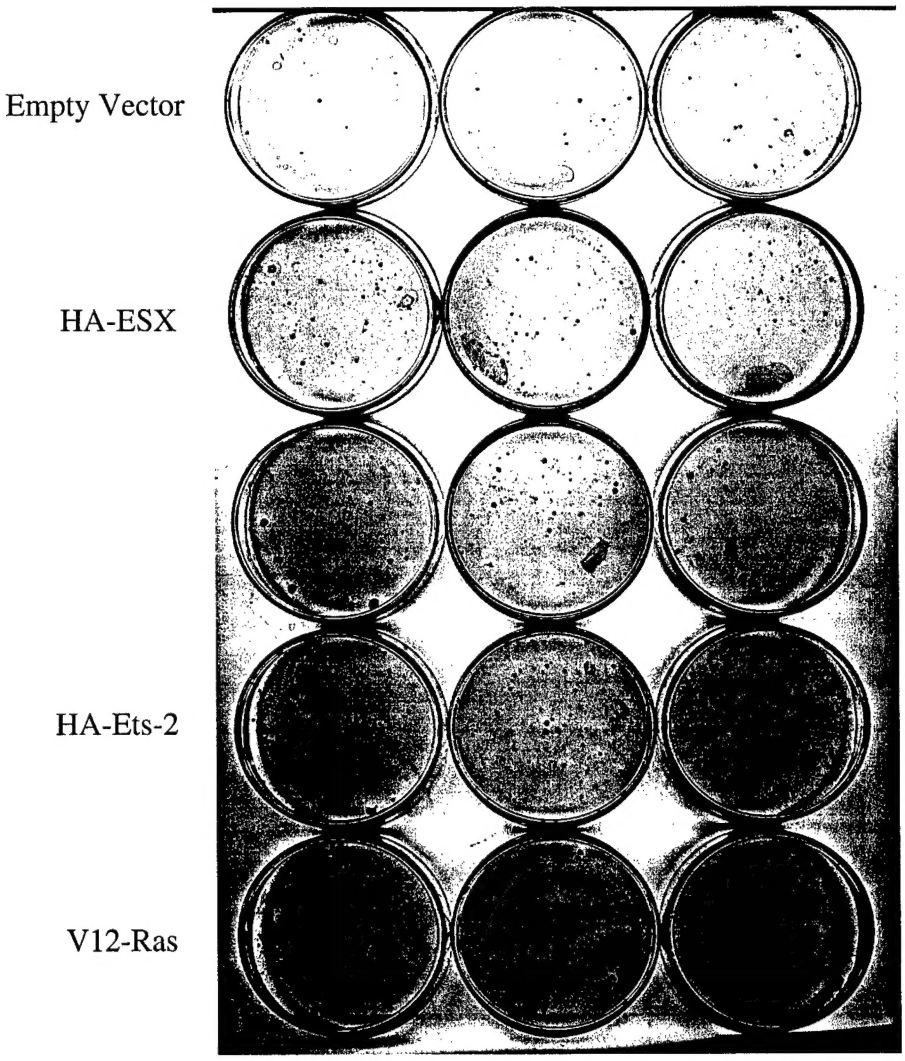

Figure 8

Table 1

Foci induction in MCF-12A cells by Ets factors[+]

Empty Vector	**HA-ESX**	**HA-VP16-ESX**	**HA-Ets-2**	**V12-Ras**
6(±3)	17(±6)	20(±5)	23(±17)	32(±8)

[+]Triplicate results shown in Fig 8B were counted (colonies ≥ 1 mm) and the average number of foci per plate ± S.D. are tabulated.

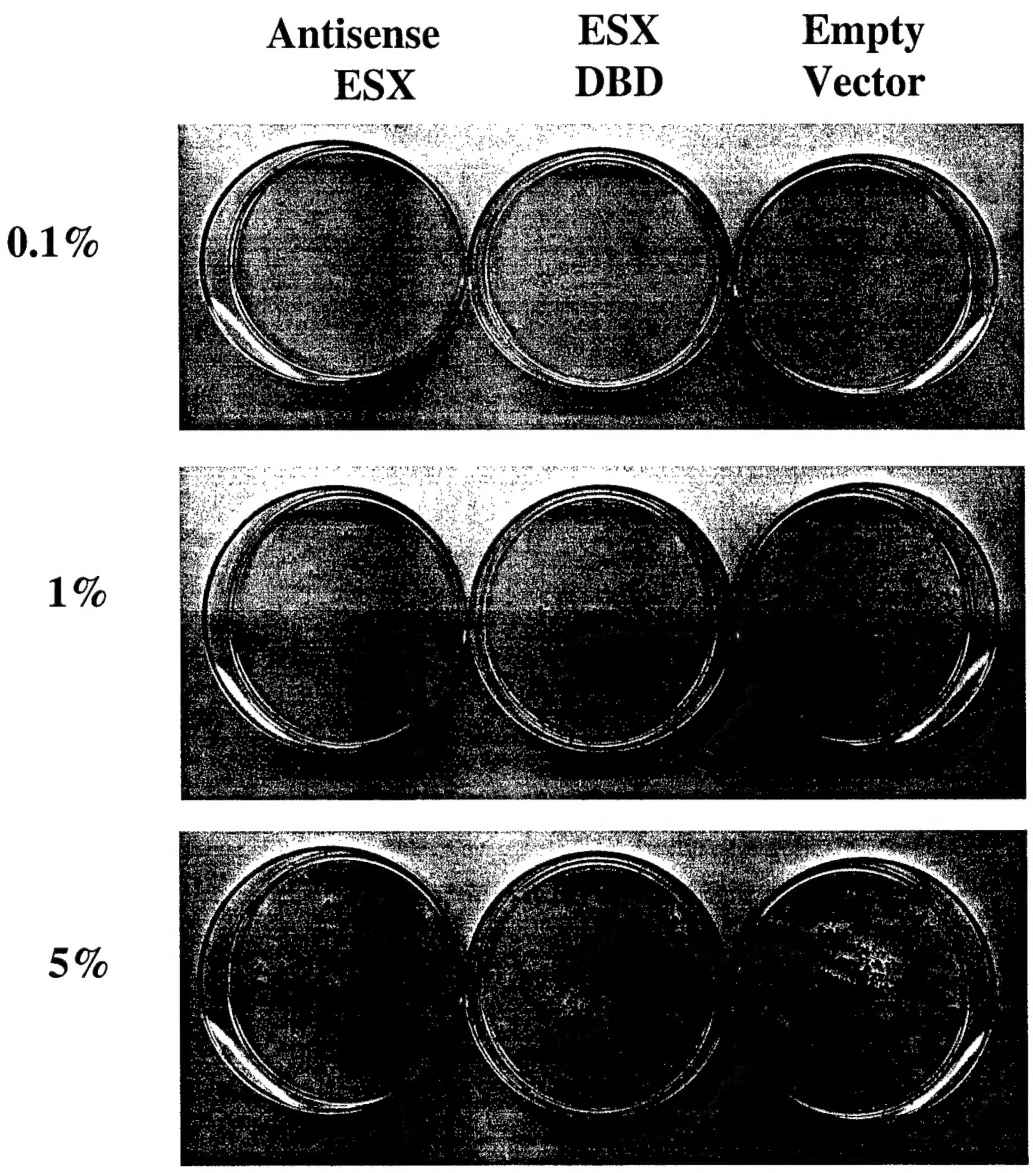

Figure 9

Table 2

Inhibition of T47D foci formation by inhibitory ESX constructs[+]

% FCS	**HA-antisense-ESX**	**HA-ESX DBD**	**Empty Vector**
0.1	67 (22%)*	52 (17%)	303
1	82 (28%)	67 (22%)	301
5	126 (39%)	146 (45%)	326

[+]Triplicate results shown in Fig 9 were counted and the average number of foci per plate is tabulated.

*Numbers in paranthesis represent the % of total foci formed by empty vector.